

Portland State University

**PDXScholar**

---

Geology Faculty Publications and Presentations

Geology

---

4-7-2021

# Glaciers of the Olympic Mountains, Washington - The Past and Future 100 Years

Andrew G. Fountain

*Portland State University, andrew@pdx.edu*

Christina Gray

*Portland State University*

Bryce Allen Glenn

*Portland State University, brglenn@pdx.edu*

Brian Menounos

*University of Northern British Columbia*

Justin Pflug

*University of Northern British Columbia*

*See next page for additional authors*

Follow this and additional works at: [https://pdxscholar.library.pdx.edu/geology\\_fac](https://pdxscholar.library.pdx.edu/geology_fac)



Part of the [Geology Commons](#)

**Let us know how access to this document benefits you.**

---

## Citation Details

Published as: Fountain, A. G., Gray, C., Glenn, B., Menounos, B., Pflug, J., & Riedel, J. L. (2022). Glaciers of the Olympic Mountains, Washington—The past and future 100 years. *Journal of Geophysical Research: Earth Surface*, 127, e2022JF006670. <https://doi.org/10.1029/2022JF006670>

This Post-Print is brought to you for free and open access. It has been accepted for inclusion in Geology Faculty Publications and Presentations by an authorized administrator of PDXScholar. Please contact us if we can make this document more accessible: [pdxscholar@pdx.edu](mailto:pdxscholar@pdx.edu).

---

**Authors**

Andrew G. Fountain, Christina Gray, Bryce Allen Glenn, Brian Menounos, Justin Pflug, and Jon L. Riedel

1  
2 **Glaciers of the Olympic Mountains, Washington**  
3 **– the past and future 100 years**  
4

5 **Andrew G. Fountain<sup>1</sup>, Christina Gray<sup>1</sup>, Bryce Glenn<sup>1</sup>, Brian Menounos<sup>2</sup>, Justin Pflug<sup>2</sup> Jon L.**  
6 **Riedel<sup>3</sup>**  
7

8 <sup>1</sup>Department of Geology, Portland State University, Portland, Oregon, USA  
9

10 <sup>2</sup>Geography Program, University of Northern British Columbia, 3333 University Way, Prince George, British  
11 Columbia Canada  
12

13 <sup>3</sup>Department of Civil and Environmental Engineering, University of Washington, Seattle, Washington, USA  
14

15 <sup>4</sup>US National Park Service, North Cascades National Park, 810 State Route 20, Sedro-Woolley, Washington  
16 USA  
17  
18

19 **Key Points:**  
20

- 21 • The glaciers of the Olympus Peninsula are shrinking rapidly, losing half of its ice-  
22 covered area since 1900

- 23  
24 • Warming air temperatures are causing glacier loss; warming winter temperatures  
25 change the phase of the precipitation from snow to rain.

- 26  
27 • Modeling suggests the glaciers will largely disappear by 2070  
28  
29  
30  
31  
32  
33  
34

35 Corresponding author: Andrew G. Fountain, [andrew@pdx.edu](mailto:andrew@pdx.edu)

36 **Abstract**

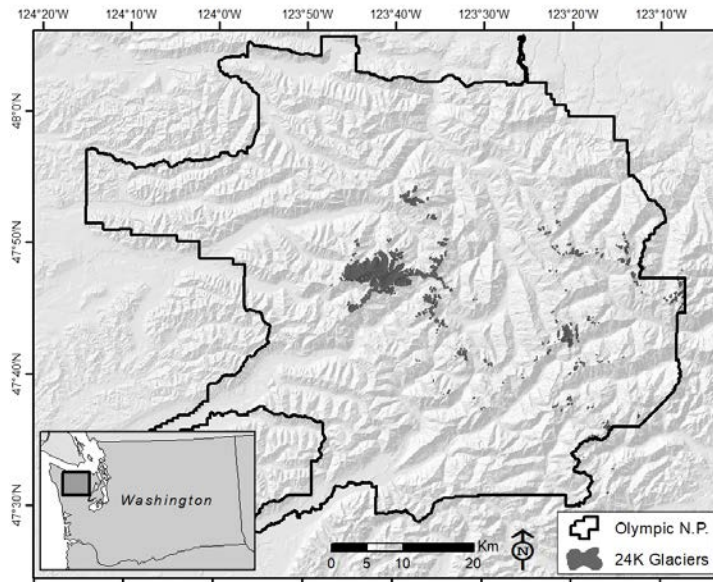
37  
38 In 2015, the Olympic Mountains contain 255 glaciers and perennial snowfields totaling  $25.34 \pm$   
39  $0.27 \text{ km}^2$ , half of the area in 1900, and about  $0.75 \pm 0.19 \text{ km}^3$  of ice. Since 1980, glaciers shrank  
40 at a rate of  $-0.59 \text{ km}^2 \text{ yr}^{-1}$  during which 35 glaciers and 16 perennial snowfields disappeared.  
41 Area changes of Blue Glacier, the largest glacier in the study region, was a good proxy for  
42 glacier change of the entire region. A simple mass balance model of the glacier, based on  
43 monthly air temperature and precipitation, correlates with glacier area change. The mass  
44 balance is highly sensitive to changes in air temperature rather than precipitation, typical of  
45 maritime glaciers. In addition to increasing summer melt, warmer winter temperatures changed  
46 the phase of precipitation from snow to rain, reducing snow accumulation. Changes in glacier  
47 mass balance are highly correlated with the Pacific North American index, a proxy for  
48 atmospheric circulation patterns and controls air temperatures along the Pacific Coast of North  
49 America. Regime shifts of sea surface temperatures in the North Pacific, reflected in the Pacific  
50 Decadal Oscillation (PDO), trigger shifts in the trend of glacier mass balance. Negative ('cool')  
51 phases of the PDO are associated with glacier stability or slight mass gain whereas positive  
52 ('warm') phases are associated with mass loss and glacier retreat. Over the past century the  
53 overall retreat is due to warming air temperatures, almost  $+1^\circ\text{C}$  in winter and  $+0.3^\circ\text{C}$  in  
54 summer. The glaciers in the Olympic Mountains are expected to largely disappear by 2070.

55  
56

57 **1. Introduction**

58  
59 The Olympic Mountains are the western-most alpine terrain in the Pacific Northwest US,  
60 isolated on the Olympic Peninsula of Washington State. These mountains are first to intercept  
61 moisture-laden storms originating over the Pacific Ocean with the highest peak (Mt. Olympus)  
62 56 km inland. Although the mountains only reach to 2432 m above sea level (asl), glaciers  
63 mantle the highest mountains due to the heavy winter snowfall and cool summers.

64 Precipitation varies from 3000 mm yr<sup>-1</sup> on the west side of the range to only 500 mm yr<sup>-1</sup> on the  
65 east (Rasmussen et al., 2001).  
66



67 *Figure 1. Location of the Olympic Peninsula and glaciers. The dark black line is the boundary of*  
68 *Olympic National Park. The gray outlined box surrounds Mt. Olympus.*

69

70 Glaciers were first photographed in 1890 during a US Army Exploring Expedition (Spicer, 1989;  
71 Wood, 1976). One glacier, the Blue Glacier, became the focus of interest because it is the  
72 largest glacier in the region. During the International Geophysical Year in 1957 it was mapped  
73 and identified as one of the glaciers in western North America suitable for monitoring (AGS,  
74 1960). In that same year a mass balance monitoring program was established and has  
75 continued intermittently (Armstrong, 1989; Conway et al., 1999; LaChapelle, 1959).

76 Spicer (1986) compiled the first detailed inventory of the region. He mapped the glaciers by  
77 modifying glacier outlines on US Geological Survey 1:36,360-scale topographic maps according  
78 to their extent on vertical aerial photographs (1:24,000 to 1:60,000) acquired in 1976, 1979,  
79 1981, and 1982, and supported by field observations from 1980 - 1983. Ice masses were  
80 classified as glaciers if they persisted for at least two years; displayed evidence of glacier flow

81 such as crevasses, medial moraines, meltwater with glacier flour; or showed glacial activity such  
82 as terminal or lateral moraines.

83

84 Fountain et al. (2017) developed a second inventory of glaciers and perennial snowfields in the  
85 Olympic Mountains as part of a larger inventory that included the entire western US exclusive  
86 of Alaska. The outlines of this newer inventory were abstracted from US Geological Survey  
87 1:24,000-scale topographic maps drawn from aerial photography flown in 1943, 1968, 1976,  
88 1979, 1985, and 1987. Most glaciers (93%) were photographed during 1985-1987 and only a  
89 few in 1943. This inventory identified more glaciers (391) than Spicer (265) largely due to  
90 Spicer's 0.1 km<sup>2</sup> area threshold for inclusion, compared to the 0.01 km<sup>2</sup> adopted by Fountain et  
91 al. (2017). When the 0.1 km<sup>2</sup> threshold was applied to Fountain et al. (2017) the distributions of  
92 both inventories largely accord. Riedel et al. (2015) compiled a third inventory of glaciers based  
93 on aerial photography from 2009. One of the authors (Fountain) was involved with the  
94 compilation of this inventory the details of which are summarized in Methods below.

95

96 Our objectives are to provide a comprehensive examination of the glaciers in the Olympic  
97 Mountains, how they have changed in area and volume since the early 1980s to 2015, and how  
98 they responded to climatic variations since 1900. This report differs from Riedel et al. (2015) in  
99 several ways. First, we provide two new inventories and examine in detail how the populations  
100 change over time. We demonstrate that area changes of Blue Glacier are representative of the  
101 population as a whole and examine the precipitation and air temperature influences on Blue  
102 Glacier in the context of larger climate indices that represent hemispheric scale oceanic and  
103 atmospheric processes. Finally, we predict the future of glacier cover in the Olympics over the  
104 next century.

105

## 106 **2. Methods**

107 To assess the changing area and distribution of glaciers in the Olympic Mountains we relied on  
108 several previously published glacier inventories and created two new inventories. The first  
109 glacier inventory from Spicer (1986) provides the earliest detailed inventory, however, results

110 are in tabular form with approximate latitude and longitude locations. Newer inventories were  
111 compiled in a geographic information system as digital outlines of glaciers and perennial  
112 snowfields. Three new inventories were compiled for the Olympic Mountains using vertical  
113 aerial photographs flown in September of 1990, 2009, and 2015. The 1990 images are black and  
114 white digital orthoquadrangles (DOQs) with a ground resolution of 1 m. They were downloaded  
115 from the University of Washington Geomorphological Research Group webpage (UW, 2019).  
116 The 2009 and 2015 imagery were obtained from the U.S. Department of Agriculture (USDA)  
117 National Agricultural Imagery Program (NAIP) website (USDA, 2019) as 1 m color georectified  
118 orthophotographs. The 2009 inventory was reported in Riedel et al (2015). The 2015 imagery  
119 included all but 16 glaciers, which were outlined using WorldView-2 satellite imagery, 0.5 m  
120 spatial resolution obtained from Digital Globe and acquired in August and September (Gorelick  
121 et al., 2017). The comprehensive inventory of the continental US (Fountain et al., 2007, 2017)  
122 was not used because the original USGS imagery of the Olympic Mountains included extensive  
123 seasonal snow masking many of the glacier outlines. Also, the imagery dates are within a couple  
124 of years of Spicer's inventory rendering the inventory unnecessary.

125  
126 The new inventories include both glaciers and perennial snowfields (G&PS) because they are  
127 often hard to distinguish when small and perennial snowfields can be locally important for late  
128 summer runoff (Clow & Sueker, 2000; Elder et al., 1991). Glaciers are identified by the presence  
129 of exposed ice and crevasses, indicating a perennial nature and movement, respectively.  
130 Snowfields, on the other hand, rarely provide visual clues regarding their perennial nature  
131 because their firn core is usually snow-covered in the imagery. We only track their persistent  
132 presence in the imagery. Given the episodic nature of suitable imagery over four decades these  
133 features cannot be tracked closely. Therefore, we adopt rules from (DeVisser & Fountain, 2015)  
134 to distinguish seasonal from perennial features. In short, if a feature is present in the first  
135 inventory (Spicer for glaciers, 1990 for snowfields) and not found in subsequent inventories it is  
136 considered seasonal and eliminated. If the feature is found in the first two inventories it is  
137 considered perennial, and if it is absent from any subsequent inventory it is considered no  
138 longer perennial. Outlines were digitized in ArcGIS (ArcMap, ESRI, Inc) at a scale of 1:2,000 with

139 vertices spaced at a 5 m interval. This approach balanced accuracy, productivity, and image  
140 resolution. The minimum area threshold was 0.01 km<sup>2</sup>, consistent with Fountain et al. (2017)  
141 for the Western US, and global guidelines for glacier inventories (Paul et al., 2010). To insure  
142 internal consistency, the three new inventories were intercompared and any abrupt change in  
143 area initiated a reexamination of that G&PS outline.

144  
145 Area uncertainty results from three sources, positional, digitizing, and interpretation (DeBEER &  
146 Sharp, 2009; DeVisser & Fountain, 2015). Positional uncertainty ( $U_p$ ) is the error in the location  
147 of the perimeter caused by alignment of the base image during the orthorectification process.  
148 Digitizing uncertainty ( $U_d$ ) results from inaccuracies in following the glacial perimeter during  
149 manual digitizing. Finally, interpretation uncertainty ( $U_i$ ) is the location uncertainty of the  
150 glacier margin due to masking by seasonal snow cover, rock debris, or shadows. The total  
151 uncertainty ( $U_t$ ) for each feature is the square root of the sum of the square of each  
152 contributing uncertainties (Baird, 1962).

153  
154 
$$U_t = \sqrt{U_p^2 + U_d^2 + U_i^2} \quad (1)$$

155  
156 To evaluate (1), we ignored positional uncertainty ( $U_p$ ) because we are concerned with area not  
157 exact location. Furthermore, the digitized points are highly correlated such that they are not  
158 independently determined. To evaluate the digitization uncertainty ( $U_d$ ), we follow (Hoffman et  
159 al., 2007) who adapted the method of (Ghilani, 2000). This uncertainty is a product of the  
160 length of the side of a square ( $S$ ) that has the same area as the feature polygon in question  
161 multiplied by the linear uncertainty ( $\sigma_d$ ),

162  
163 
$$U_d = S\sigma_d\sqrt{2} \quad (2)$$

164  
165 To estimate the linear uncertainty ( $\sigma_d$ ). Ten features of various sizes were digitized at the  
166 normal 1:2000 scale and again at 1:500. The linear difference was measured perpendicularly  
167 between outlines and the standard deviation calculated. For interpretation uncertainty we tried

168 several approaches including, visual estimates (e.g. 5% of the area is in shadow, uncertainty is  
169  $\pm 2.5\%$ ), measured glacier area with and without the questionable subregion using one half of  
170 the difference as the uncertainty, or a combination of both approaches where measurements  
171 were used to calibrate visual estimates. In most cases we found little difference between  
172 methods.

173

174 The uncertainty for snowfields was estimated differently. Snowfield area commonly changed  
175 dramatically ( $\sim 50\%$ ) between imagery surveys, due to residual seasonal snow. Because its firn  
176 core was rarely observed uncertainty is unknown. To document the presence of perennial  
177 snowfields but eliminate them from analysis, a large uncertainty was estimated using a buffer  
178 around the outline such that the observed changes in area were smaller than the uncertainty.

179

180 To calculate the topographic characteristics of the initial, (Spicer, 1986) inventory, we used the  
181 original National Elevation Dataset based on the 1:24,000 paper maps (Gesch et al., 2002).

182 Most of the mapping (94%) in the Olympics was based on aerial photography from 1980-1987  
183 (Fountain et al., 2017). As will be shown later, during this period little glacier recession occurred  
184 and we consider the topography to be representative of the 1980 inventory.

185

186 Volume change was estimated by differencing surface elevations of the glaciers collected at  
187 different times. Two digital elevation models (DEMs) were used. The earlier DEM is the National  
188 Elevation Dataset and the more recent DEM is from aerial lidar collected in summer 2015  
189 (Painter et al., 2016). Uncertainty was estimated by the root-mean square error of the elevation  
190 differences calculated for the snow-free bedrock adjacent to the glaciers.

191

192 The local climate of precipitation and maximum/minimum air temperatures was defined using  
193 Parameter-elevation Regression on Independent Slopes (PRISM) data (Daly et al., 2007).

194 Monthly values were downloaded at a scale of 4 km within a box 10.7 km by 8.5 km, centered  
195 over Mt. Olympus ( $47.7986^\circ$ ,  $-123.693^\circ$ ) (OSU, 2017). To examine the influence of broader  
196 climate patterns climate indices were downloaded from a number of sources. For the Arctic

197 Oscillation (AO, Barnston and Livezey, 1987; Thompson and Wallace, 1998); Nino 3.4 (Bjerknes,  
198 1966; Rayner et al., 2003; Trenberth, 1997); North Atlantic Oscillation (NAO, Jones et al., 1997);  
199 North Pacific index (Trenberth & Hurrell, 1994); Pacific-North American (PNA, Wallace &  
200 Gutzler, 1981), and the Southern Oscillation Index (Cayan, 1996; Chen, 1982; Ropelewski &  
201 Jones, 1987), the data were downloaded from the US National Oceanic and Atmospheric  
202 Administration, Earth System Research Laboratory, Physical Sciences Division (NOAA, 2018).  
203 The data for the Pacific Decadal Oscillation (PDO, Mantua & Hare, 2002; Newman et al., 2016),  
204 were downloaded from the University of Washington (UW, 2018). The period of correlation was  
205 1900 – 2014 for all variables except Arctic Oscillation, which was 1950-2014 due to data  
206 availability. The correlations reported are for the longer period of record.

207

### 208 **3. Results**

209

210 The Spicer (1986) inventory identified 266 glaciers  $\geq 0.01 \text{ km}^2$ , most (94%) of which were  
211 identified from 1979-1982. During this period the glaciers changed little because it coincides  
212 with the mid-century cool period when glaciers were either in equilibrium or advancing slightly  
213 (Conway et al., 1999; Hodge et al., 1998; Thompson et al., 2010). For simplicity, the inventory is  
214 dated to 1980 and referred to as the '1980 inventory'. Our reanalysis revised the 1980  
215 inventory to 261 glaciers because one glacier, White Glacier, was counted as two glaciers due to  
216 its split terminus into two lobes, and four other features were considered seasonal because  
217 they were missing from the following 1990 inventory. Total glacier area was  $45.89 \pm 0.51 \text{ km}^2$ ,  
218 of which almost half,  $20.4 \text{ km}^2$ , are located on the Olympus Massif. The largest glacier was Blue  
219 Glacier,  $6.02 \pm 0.30 \text{ km}^2$  and the smallest was an unnamed ice mass,  $0.01 \text{ km}^2$ . Average glacier  
220 area was  $0.18 \text{ km}^2$  with a median of  $0.05 \text{ km}^2$ . The area of many glaciers cannot be quantified  
221 because Spicer's inventory often grouped small glaciers within the same watershed under a  
222 single identification number and summing their area. Mean glacier elevations range from 1319  
223 m to 2399 m amsl with a mean elevation of 1726 m. The mean elevation of almost all glaciers  
224 (98%) was  $< 2000 \text{ m}$  and 45% have a maximum elevation  $< 2000 \text{ m}$  (Figure 2). Glaciers facing  
225 north ( $330^\circ$  to  $30^\circ$ ) account for 55.6% of the population and 52% ( $24.0 \text{ km}^2$ ) of the total area.

226

227 The glaciers were inventoried again using imagery from 1990, 2009, and 2015. These were the  
228 years with suitable late-summer imagery. The quality was good to excellent with moderate  
229 amounts of snow cover in some places. The summer of 2015 was a particularly low snow year  
230 and the alpine landscape was largely snow-free. The root mean square error of uncertainty for  
231 all outlines in each inventory was 1% of the total area. Forty-seven more G&PS were identified  
232 in the new inventories compared to the original 1980 glacier inventory. GIS methods and  
233 comparison between inventories more conclusively defined perennial features (Table 1).

234

235

236

237

238

239

240

241

242

243

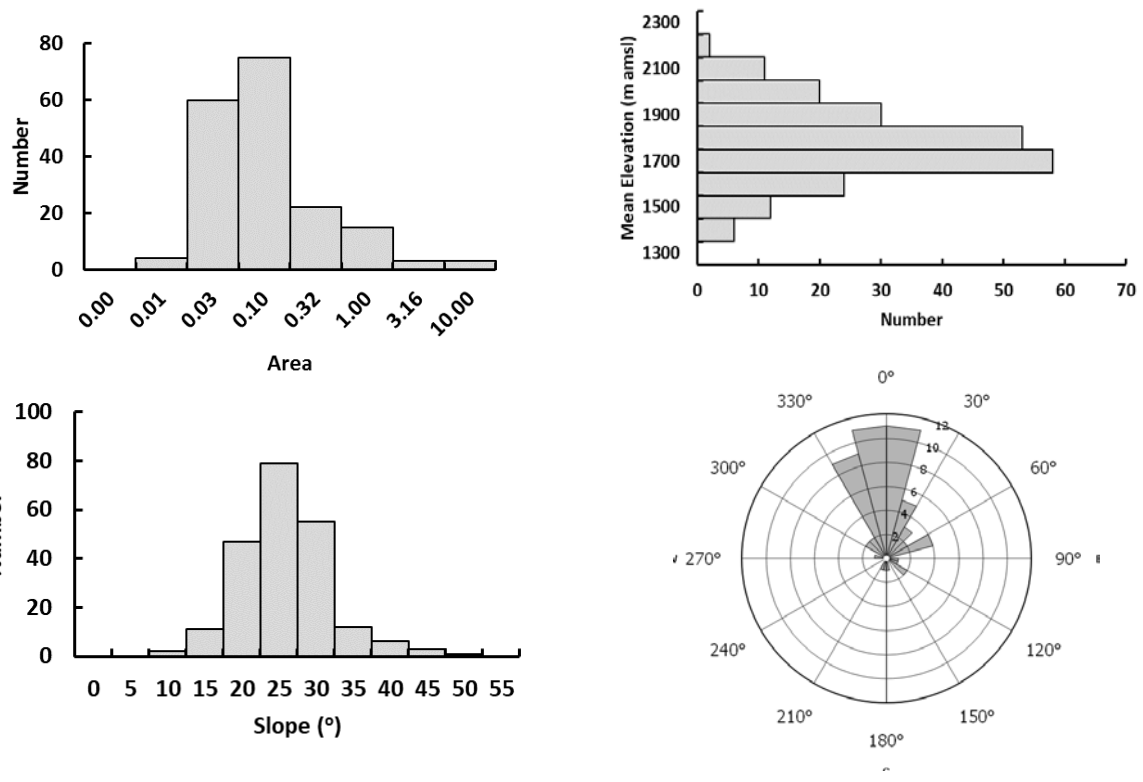
244

245

246

247

248



249 *Figure 2. Topographic characteristics of the 1980 glacier inventory. Clockwise from upper left:*  
250 *Frequency distributions of glacier area, mean elevation, aspect, and mean slope. For bar graphs,*  
251 *the value of the bin is the maximum value for bin. For area, note the logarithmic values on the x-*  
252 *axis.*

253

254 Tracking the glaciers originally identified by the 1980 inventory showed that by 2015, total  
255 glacier area decreased by -45% ( $-0.59 \text{ km}^2 \text{ yr}^{-1}$ ), mean glacier area decreased from  $0.18 \text{ km}^2$  to  
256  $0.10 \text{ km}^2$ , and 35 glaciers disappeared (Table 1 Partial Inventory). The distribution of glacier  
257 area in 1980 approximates a normal distribution, but becomes increasingly skewed favoring  
258 smaller glaciers with time resulting in a highly skewed area-population distribution by 2015  
259 (Figure 3). Given the close correspondence of fractional area change between the complete and  
260 partial inventories, we estimate that about 45% of the ice-covered area was lost between 1980  
261 and 2015. A total of 51 G&PS in the complete inventory disappeared and 134 decreased below  
262  $0.01 \text{ km}^2$  (but  $> 0$ ), the minimum threshold for glacier inclusion (Fountain et al., 2017; Paul et  
263 al., 2010). These very small ice masses remain in the inventory given their perennial nature and  
264 their known history.

265

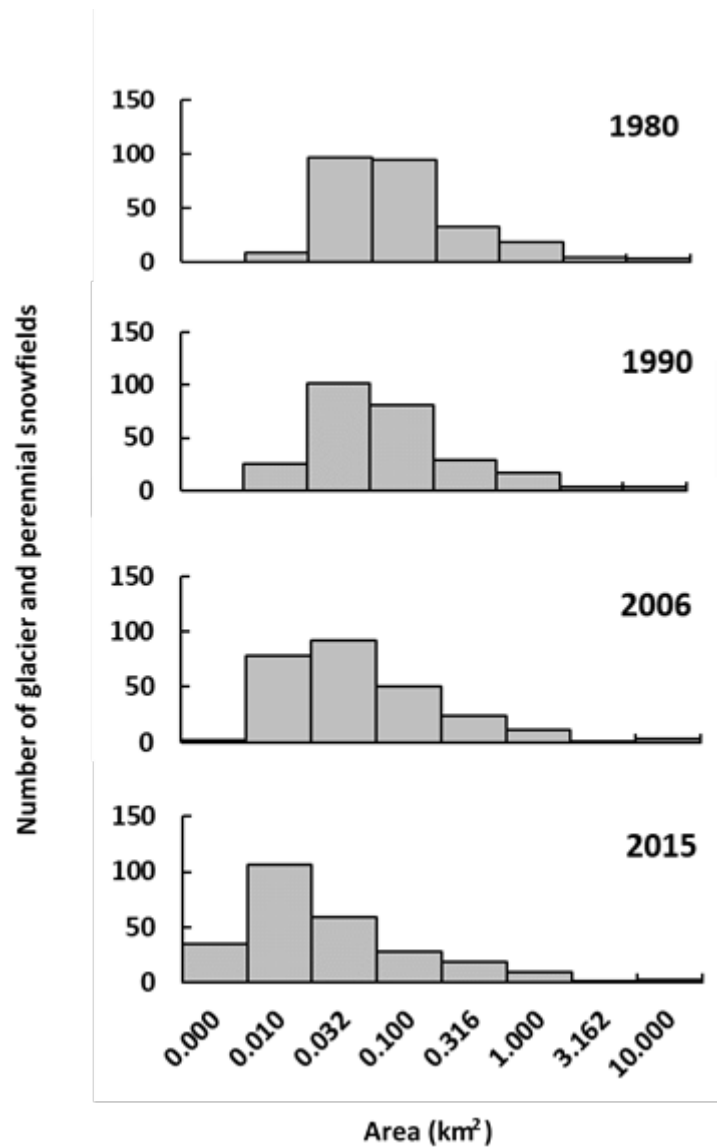
266 The time periods between inventories vary from 6 to 19 years, during which 19% - 37% of area  
267 changes were less than the uncertainty. During every time period total glacier area decreased,  
268 but with one to eight glaciers increased area greater than uncertainty. No glacier increased area  
269 for two or more consecutive time periods. The rate of total area change slowed from  $-0.66 \text{ km}^2$   
270  $\text{yr}^{-1}$  (1980-1990) to about  $-0.48 \text{ km}^2 \text{ yr}^{-1}$  (1990-2009) before accelerating again to  $-0.82 \text{ km}^2 \text{ yr}^{-1}$   
271 (2009-2015). Of the G&PS that disappeared, most occurred in the last period, 1990-2009.

272

273 *Table 1. Statistics for inventories of all glaciers and perennial snowfields found in the Olympic Mountains.*  
274 *The Complete Inventory summarizes all glaciers found in each inventory and the Partial Inventory are*  
275 *those that are common to the 1980 inventory. For area and uncertainty ( $\text{km}^2$ ), Max is maximum, Min is*  
276 *minimum, Med, is median area. Area change is the change since last inventory and can only be*  
277 *calculated for inventories that include the same populations; R Frc Chg is the relative fractional area*  
278 *change since previous inventory and is the change (and uncertainty) divided by the area of the previous*  
279 *inventory; T Frc Chg is the total fractional change since the 1980 inventory; Rate Chg is the rate of area*  
280 *change in  $\text{km}^2 \text{ yr}^{-1}$  based on the area change and years between inventories; Total Num is the number of*  
281 *glaciers and perennial snowfields in the inventory; Disappeared is the number that have vanished since*  
282 *last inventory. Uncertainty is included in smaller font, and is the root mean square error except for the*

283 mean, which is the standard deviation. The 2009 inventory was originally published in Riedel et al (  
 284 2015).

	1980	1990	2009	2015
<b>Complete Inventory</b>				
Max Area	6.02 ± 0.30	5.74 ± 0.30	5.35 ± 0.08	5.14 ± 0.09
Min Area	0.01 ± 0.00	0.001 ± 0.001	0.000 ± 0.000	0.000 ± 0.000
Mean Area	0.18 ± 0.59	0.13 ± 0.51	0.10 ± 0.46	0.08 ± 0.43
Med. Area	0.05	0.02	0.01	0.01
Total Area	45.89 ± 0.51	39.66 ± 0.53	30.35 ± 0.22	25.34 ± 0.27
Area Chg			-9.31 ± 0.58	-5.01 ± 0.35
R. Frc. Chg			-0.23 ± 0.01	-0.17 ± 0.01
T. Frc. Chg			-0.23 ± 0.01	-0.36 ± 0.02
Rate Chg			-0.49 ± 0.03	-0.84 ± 0.06
Total Num	261	308	306	255
Disappeared		0	2	51
<b>Partial Inventory</b>				
Max Area	6.02 ± 0.30	5.74 ± 0.30	5.35 ± 0.08	5.14 ± 0.09
Min Area	0.01 ± 0.00	0.001 ± 0.001	0.000 ± 0.000	0.000 ± 0.000
Mean Area	0.18 ± 0.59	0.15 ± 0.55	0.12 ± 0.49	0.10 ± 0.47
Med. Area	0.05	0.03	0.02	0.01
Tot. Area	45.89 ± 0.51	39.31 ± 0.53	30.16 ± 0.22	25.25 ± 0.27
Area Chg		-6.58 ± 0.74	-9.15 ± 0.58	-4.90 ± 0.35
R. Frc. Chg		-0.14 ± 0.02	-0.23 ± 0.01	-0.16 ± 0.01
T. Frc. Chg		-0.14 ± 0.02	-0.34 ± 0.01	-0.45 ± 0.02
Rate Chg		-0.66	-0.48 ± 0.03	-0.82 ± 0.02
Total Num	261	261	259	226
Disappeared		0	2	35



285

286 *Figure 3. The number of glaciers as a function of their area for each of the inventories. The*  
 287 *horizontal axis intervals are logarithmic increasing by a power of 0.5; tick labels on the x-axis*  
 288 *represents maximum bin value. The G&PS in the zero column are those that disappeared since*  
 289 *the previous inventory.*

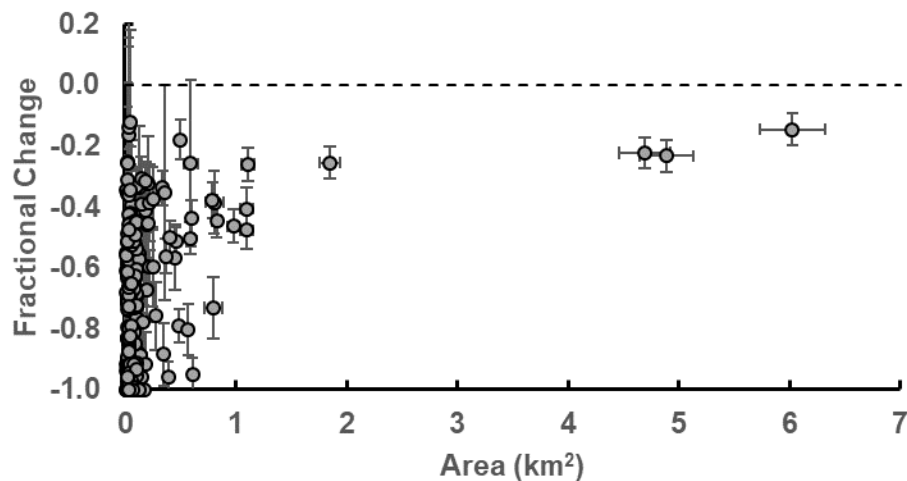
290

#### 291 **4. Analysis**

292

##### 293 **4.1 Effect of Topography**

294 To examine the influence of topographic factors, such as elevation and aspect, on glacier  
295 area change, the change was first normalized by dividing by initial area yielding a fractional  
296 area change. Results show that smaller glaciers shrink proportionally more than larger  
297 glaciers but the variability of shrinkage is also much larger. Much of the variability in very  
298 small glaciers is probably due to local topographic effects, such as topographic shadowing  
299 by valley walls or local snow accumulation via avalanching and wind drift (Basagic &  
300 Fountain, 2011; DeBEER & Sharp, 2009; Kuhn, 1995). In contrast, local boundary conditions  
301 affect larger glaciers much less. In order to minimize boundary effects, the glaciers  $<0.1 \text{ km}^2$   
302 were eliminated from the topographic analysis.  
303



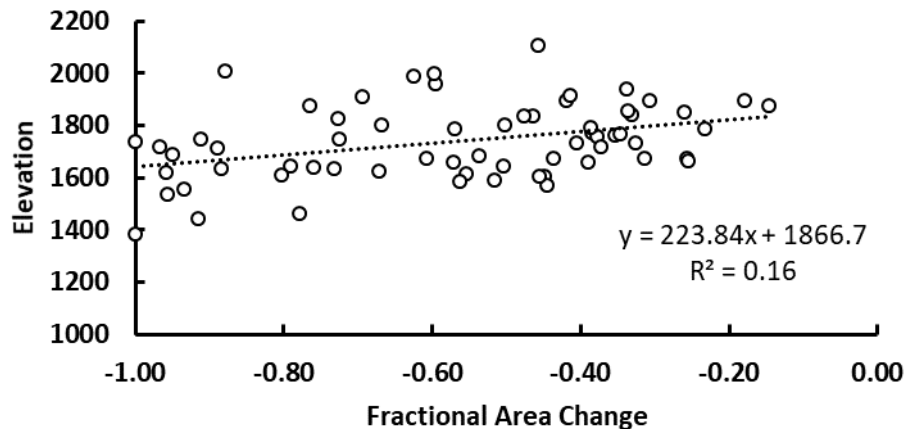
304 *Figure 4. Fractional area change of the glaciers and perennial snowfields in the Olympic*  
305 *Mountains as a function of initial area from 1980 to 2015 using the only the glaciers identified in*  
306 *1980.*

307  
308 No correlation of fractional area change was found with area, aspect, slope, distance from the  
309 Pacific Ocean, winter precipitation or average seasonal temperature (summer, winter). The only  
310 correlative factor was elevation (Figure 5). Area changes were further examined by sorting the  
311 entire data set, including the small G&PS, from greatest to least, then subdivided into four  
312 groups. The topographic and climatic characteristics of the group with the largest change ( $\geq -$

313 92%) were compared to those of the smallest change ( $\leq -51\%$ ). Each group consisted of about  
314 55 glaciers. For glaciers with the largest relative change, almost half (21) disappeared, had a  
315 lower maximum elevation ( $\Delta -250$  m). Although no significant differences were observed for the  
316 other variables, the glaciers with the largest fractional change tended to be smaller (mean of  
317  $0.06 \text{ km}^2$  versus  $0.56 \text{ km}^2$ ), and warmer ( $\Delta +0.7^\circ\text{C}$ ) air temperature in summer and winter,  
318 consistent with a lower elevation (Table A1).

319  
320 To examine the effect of the distribution of glacier area with elevation the hypsometry index  
321 was compared with fractional area change. The index is a ratio of the elevation differences  
322 between the maximum and median and the median and minimum (Jiskoot et al., 2009). For  
323 example, if the elevation difference above the median is smaller than below the median it  
324 implies a shallow broad accumulation zone compared to a longer, narrower ablation zone. We  
325 expected that glaciers with a greater elevation extent above the median than below exhibit less  
326 area change over time. No pattern was found; accounting for aspect, elevation, or local climate  
327 provided no improvement.

328  
329  
330



331  
332 *Figure 5. The fractional area change (1980 to 2015) of glaciers and perennial*  
333 *snowfields ( $>0.1 \text{ km}^2$ ) with elevation.*

334

335 4.2 Volume Change

336

337 The SnowEx lidar surveyed 216 of 261 glaciers (83%) identified by 1980 inventory. In terms of  
338 that inventory those 216 glaciers account for 43.0 km<sup>2</sup> (94%) of the total 45.9 km<sup>2</sup> area. The  
339 estimated volume change between 1980 and 2015 is  $-0.694 \pm 0.164$  km<sup>3</sup> with a specific average  
340 volume change of  $-16.1 \pm 3.8$  m. If this average is applied to the 45 glaciers not included in the  
341 lidar survey, the total estimated volume change is  $-0.741 \pm 0.164$  km<sup>3</sup>. No significant spatial  
342 trends were observed with mean glacier elevation, slope, latitude, or longitude. If we assume  
343 that all mass loss from storage occurs during the months of August and September, the period  
344 in which seasonal snow is at a minimum and maximum ice is exposed, then the contribution to  
345 stream runoff is about  $347,000 \pm 77,000$  m<sup>-3</sup> dy<sup>-1</sup>.

346

347 We estimated the remaining ice volume in 2015 using an area – volume scaling relation (Bahr et  
348 al., 2015). For glacier area, S, the volume, V, can be estimated as,

349

350 
$$V = cS^{\gamma} , \tag{1}$$

351

352 with c and  $\gamma$  as undefined parameters. We used parameter values from the literature including  
353 those based on theoretical grounds (Bahr et al., 2015) and on empirical results (Chen &  
354 Ohmura, 1990; Farinotti et al., 2009). Five estimates of volume were generated. The high and  
355 low volume estimates were eliminated and the middle three were averaged, those included  
356 Chen and Ohmura's (1990) categories of 'for the Cascades and other areas', 'for Cascades, small  
357 glaciers'; and Farinotti et al., (2009), yielding,  $0.75 \pm 0.19$  km<sup>3</sup>. The uncertainty is the standard  
358 deviation of the estimates. The Cascades refers to the mountain range ~100 km northeast of  
359 the Olympics and it has a similar climate regime. From this estimate volume and the volume  
360 change, the estimated total volume of all glaciers in 1980 is  $1.49 \pm 0.25$  km<sup>3</sup>.

361

362 4.3 Mt. Olympus

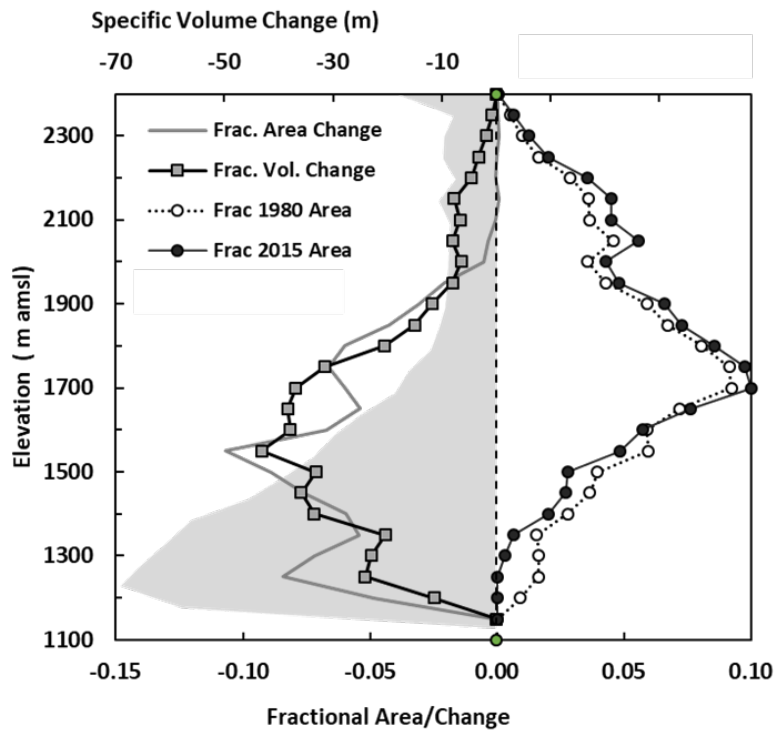
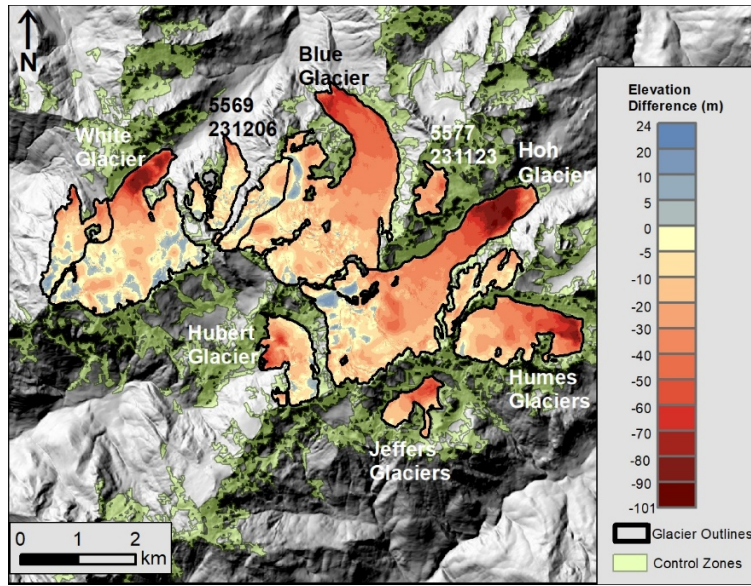
363

364 To investigate glacier change more closely we focus on the glaciers mantling Mt. Olympus, the  
365 highest peak (2,432 m) in the Olympic Mountains, representing 61% of the total glacier area in  
366 the region including the four largest glaciers and 6 of the 19 named glaciers. From 1980 to  
367 2015, the glaciers lost about 0.42 km<sup>3</sup> (61% of total, Figure 6). The specific volume change for  
368 all glaciers was  $-20 \pm 4$  m, ranging from  $-30 \pm 5$  m (Humes Glacier) to  $-6 \pm 4$  m for one of the  
369 smaller unnamed glaciers. For Blue Glacier, the largest glacier, the specific volume change was -  
370  $22 \pm 4$ m.

371

372 The distribution of glacier area shifted to higher elevations, although the elevation of maximum  
373 area, 1700-1750 m, had not changed. (Figure 6). The fractional area change with elevation  
374 generally followed the fractional volume change with maximum change (decrease) at about  
375 1500m. For elevations above about 1950 m, glacier area remained constant but thinned.  
376 Specific volume, above 1250 m shows a rapid decrease with elevation until about 1900 m  
377 where it reaches a relatively constant value of about -9 m. Below 1250 m glacier area is much  
378 smaller and some of it is debris-covered.

379



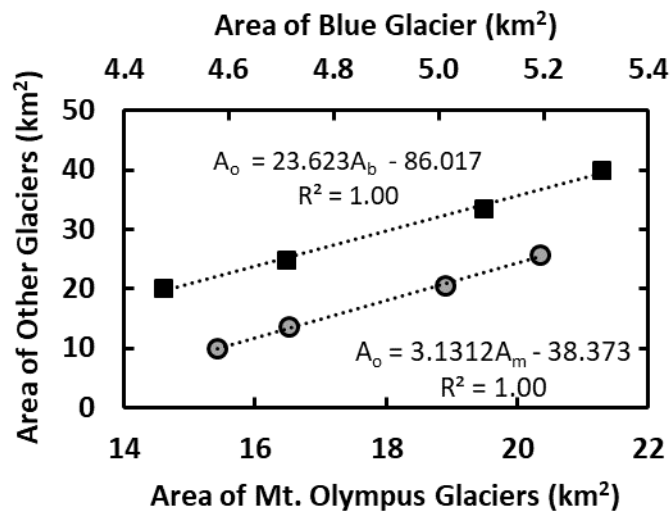
380

381

382

383 Figure 6. Area and volume changes of the glaciers n Mount Olympus (1980-2015) as a function  
 384 of elevation, in 50 m intervals. The top image shows the elevation change of all the glaciers. The  
 385 numbers identify the unnamed glaciers, the 55XX is the record number of Fountain et al. (2017)  
 386 and the 231XXX number is the hydroID of Spicer (1986). The bottom graph is the glacier change  
 387 averaged over 50 m elevation bands. Frac is the fraction of total and Vol is volume. Specific  
 388 volume change, shaded, is the volume change per unit area with an uncertainty of  $\pm 4m$ .  
 389

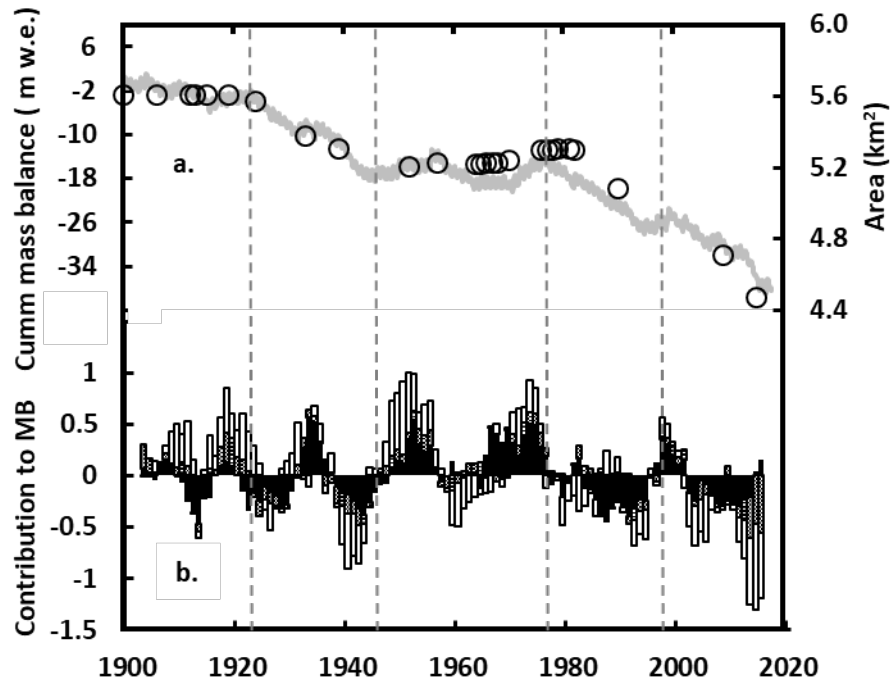
390 To test whether the changing glacier area on Mt. Olympus is representative of the other  
 391 glaciers in the region the two were compared using the compiled inventories (Figure 7). Results  
 392 show the two are highly correlated. The linear correlation suggests that should all the other  
 393 glaciers disappear the area of those on Mt. Olympus shrinks to about 12.5 km<sup>2</sup>.  
 394



395  
 396 Figure 7. Area of all the glaciers in the region, except those on Mt. Olympus, plotted with  
 397 respect to the area of the glaciers on Mt. Olympus (grey dots), and the area of all glaciers  
 398 including those on Mt. Olympus, except Blue Glacier, plotted against the area of Blue Glacier  
 399 alone (black squares). Linear regressions are shown.  $A_o$  is the area sum of all the other glaciers  
 400 in the Olympic Mountains, not including those of the independent variable.  $A_m$  is the area of all  
 401 glaciers on Mt. Olympus and  $A_b$ , the area of Blue Glacier.

402  
403  
404  
405  
406  
407  
408  
409  
410  
411  
412  
413

The most extensively studied glacier in the Olympic Mountains is Blue Glacier, dating back to the late 1950s (Conway et al., 1999; LaChapelle, 1959; Rasmussen et al., 2000; Spicer, 1989). Because of this activity and interest, the glacier area has been well-documented over time (Figure 8). The pattern shows equilibrium for the first two decades of the 20<sup>th</sup> Century, followed by rapid retreat that ended in the middle 1940s. The glacier was stable/advancing slightly over the next 40 years, peaking in the early 1980's. Note the stability in the late 1970's to early 1980's, the period of time when the Spicer and the USGS were making glacier maps of the region. By the 1990's the glaciers were in rapid retreat continuing through to 2015. Based on the correlation shown in Figure 7, the changes in the glacier area for the Olympic Mountains should vary in a similar manner. The estimated total area in 1900 is 55.3 km<sup>2</sup>, more than twice the 2015 area of 25.3 km<sup>2</sup>.



414  
415  
416  
417

Figure 8. Changes of Blue Glacier and mass balance drivers. a. Area change of Blue Glacier since 1900 (circles) and estimated cumulative (cumm) monthly mass balance (grey line). Area data prior to 1990 from Spicer (1989), see Table A2. The vertical dashed lines are climate regime

418 *shifts of the North Pacific 1923, 1946, 1977, and 1998 (see text). b. Contribution to the mass*  
419 *balance (MB) departures (5-year running mean) from winter accumulation (black), winter air*  
420 *temperature (white), and summer air temperature (cross hatched) departures*

421

#### 422 4.4 Climate Change and Glacier Mass Balance

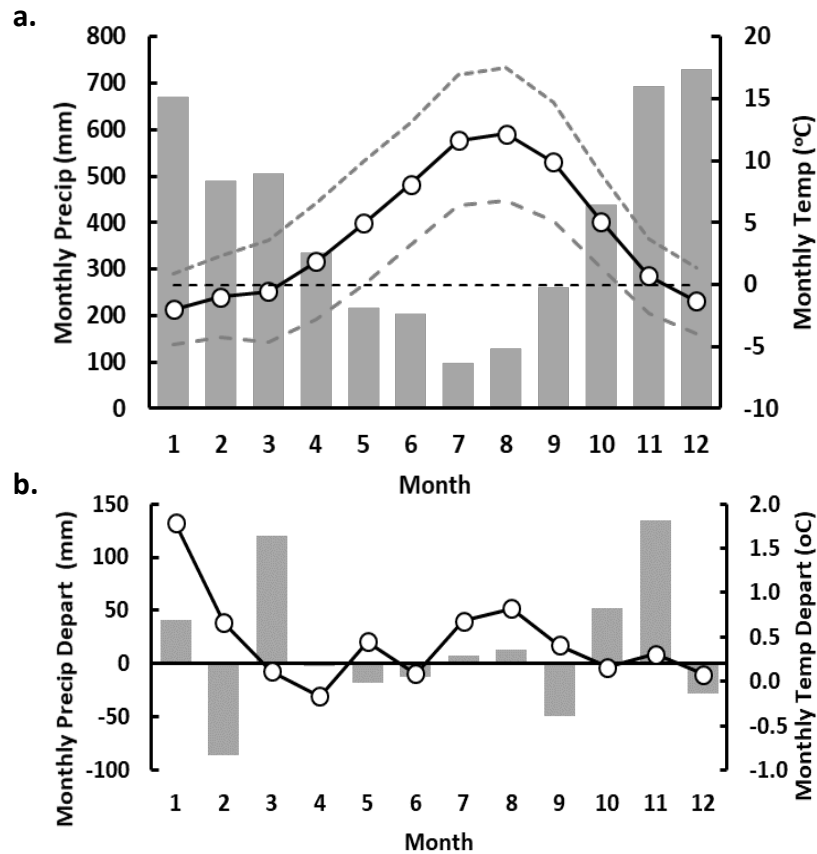
423

424 The climate of the Olympic Mountains is maritime, with relatively warm winters with abundant  
425 precipitation followed by cool dry summers (Figure 9a). The accumulation and ablation seasons  
426 were defined using air temperature. Winter was defined for those months when the minimum  
427 and mean (average of the maximum and minimum) temperatures  $< 0^{\circ}\text{C}$ ; and included  
428 December through March. Monthly maximum temperatures were commonly  $> 0^{\circ}\text{C}$ . Summer  
429 was defined for those months in which the minimum temperatures were  $\geq 0^{\circ}\text{C}$ ; and included  
430 May through October. The transition months are November and April. The net balance year  
431 nominally starts in November and ends in October.

432

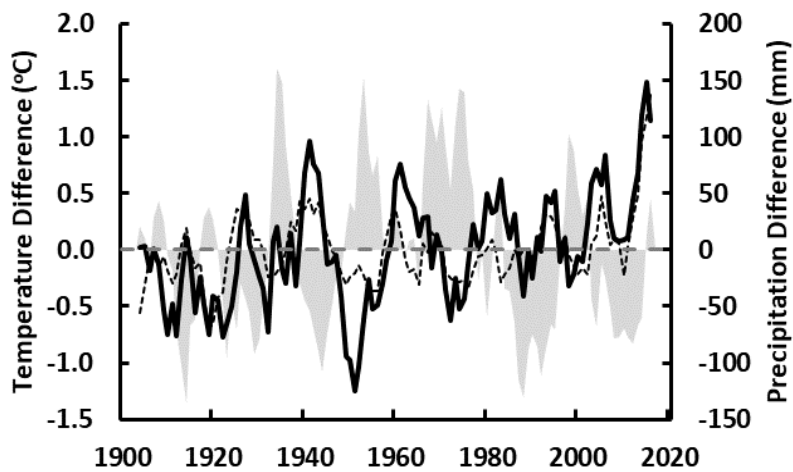
433 To determine how temperature and precipitation has changed over the past century, the  
434 monthly averages of the first 50 years of record were subtracted from the monthly averages of  
435 the last 20 years (Figure 9b). For all months, the average air temperature warmed by  $+0.5^{\circ}\text{C}$  and  
436 precipitation increased by  $+171\text{ mm}$  ( $+8\%$ ). Summer air temperatures warmed by  $+0.4^{\circ}\text{C}$  and  
437 precipitation slightly decreased  $-8\text{ mm}$  ( $-1\%$ ); for winter, temperatures warmed by  $+0.7^{\circ}\text{C}$  and  
438 precipitation increased by  $+47\text{ mm}$  ( $+2\%$ ). For specific months, monthly air temperatures  
439 warmed the most in midwinter (January,  $+1.8^{\circ}\text{C}$ ) and in mid-summer (August,  $+0.9^{\circ}\text{C}$ ).  
440 Precipitation changed little except for greater precipitation in October and November, months  
441 when the average air temperature is above freezing.

442



443 *Figure 9. Climate of the Mt. Olympus region from averaged monthly PRISM data (Daly et al.,*  
 444 *2007), (a) over period 1900 – 2017. The bars represent precipitation (precip); the gray dashed*  
 445 *and black solid curves are minimum, mean, and maximum air temperature (temp). The mean is*  
 446 *an average of the maximum and minimum values. The fine horizontal dashed line represents*  
 447 *0°C. The second panel (b) are the departures in mean temperature and monthly precipitation*  
 448 *between the average of the first 50 years of record and the last 20 years.*

449  
 450 The time series of air temperature and precipitation show a century-scale warming trend for  
 451 both summer and winter temperatures but no trend in precipitation (Figure 10). At decadal  
 452 scales both temperature and precipitation vary. Warming winter temperature is particularly  
 453 important because it is already near 0°C and further warming changes the phase of  
 454 precipitation from snow to rain, reducing snowfall (mass gain) to the glaciers.



455  
 456 *Figure 10. Difference from the mean (1900-2017) seasonal air temperature and precipitation,*  
 457 *with a 5-year running mean applied, Mt Olympus, WA. The light solid grey is winter*  
 458 *precipitation, the solid black line is winter temperature the dotted line is summer temperature.*

459  
 460 To examine how glaciers in the Olympic Mountains respond to climatic variations we use Blue  
 461 Glacier as a proxy because its area has been well-documented over the past century, its change  
 462 correlates well with regional area changes, and mass balance has been measured at the glacier  
 463 (Armstrong, 1989; Conway et al., 1999; LaChapelle, 1965). We use a simple model of glacier  
 464 mass balance to provide a more direct link to climate, rather than observed changes in area  
 465 that also responds to dynamic readjustment (Cuffey & Paterson, 2010). The model is simple and  
 466 based on monthly PRISM values of precipitation and air temperature over the entire glacier  
 467 (Daly et al., 2007; McCabe & Dettinger, 2002; McCabe & Fountain, 2013). Three adjustable  
 468 parameters are required, two of which define the phase of precipitation for snow  
 469 accumulation, the threshold temperatures for snowfall ( $\leq -2^{\circ}\text{C}$ ), and for rain ( $\geq +2^{\circ}\text{C}$ ). For  
 470 temperatures between the snow/rain thresholds the ratio linearly changes from 1 to 0.  
 471 Coincidentally, Rasmussen et al (2000) found empirically that snowfall occurred in the  
 472 accumulation zone of the glacier at air temperatures  $\leq -2^{\circ}\text{C}$ . One adjustable parameter is  
 473 required to estimate ablation and defines the rate of melt as a function of air temperature. The  
 474 monthly mass balance is then the sum of snow accumulation and ablation. We recognize the

475 limitations of this simple model, but use it here to understand the variations in mass balance,  
476 caused by changes in air temperature and precipitation, rather than for predictive values of  
477 mass balance.

478

479 Variations in the estimated mass balance closely matches the variations in glacier area over  
480 time (Figure 8). The cumulative mass balance over the period 1987-2015 is -17 m w.e. and  
481 compares favorably with the specific volume change -20 m w.e.± 4 m (-22 m ± 4 m elevation  
482 change) over the same period. Comparison with the estimated cumulative mass balance of Blue  
483 Glacier (1956-1997) by Conway et al. (1999), is good, although their mass balance increase in  
484 the 1980s was not apparent in our model. Comparisons to measured mass balances of five  
485 glaciers in the Cascade Range were also favorable in terms of synchronous change and  
486 magnitude (Riedel & Larrabee, 2016). Of the five glaciers the cumulative mass balance most  
487 closely resembled Sandalee Glacier.

488

489 Annual mass balance is best correlated with accumulation ( $R^2 = 0.98$ ) and less so with the  
490 ablation (-0.79). Accumulation is correlated equally with winter air temperature (-0.61) and  
491 winter precipitation (+0.61). Ablation, as expected, is highly and inversely correlated with  
492 annual, winter, and summer temperatures (-0.98, -0.74, -0.84, respectively). Taken together,  
493 this is suggestive of the important role of air temperature in determining mass balance with  
494 precipitation playing a secondary role. To investigate the role of air temperature further, all  
495 variables were rescaled as mean standardized departures and a multiple linear regression was  
496 calculated to predict the model mass balance from annual air temperature and winter  
497 precipitation. The regression yielded a correlation coefficient of ( $R^2 = 0.85$ ) and the correlation  
498 between the two independent variables was insignificant ( $R^2 = 0.001$ ,  $p = 0.69$ ). The relative  
499 importance of each independent variable on the mass balance was evaluated by multiplying the  
500 time series of each independent variable by its regression coefficient (McCabe & Wolock,  
501 2009). Annual air temperature accounted for 83% of the variability in the root mean square  
502 value of mass balance whereas winter precipitation accounted for 53%. The regression was run  
503 again but with three independent variables, winter precipitation, summer air temperature and

504 winter air temperature, to define which seasonal air temperature was most influential. The  
505 regression yielded a slightly lower correlation ( $R^2= 0.82$ ); and winter precipitation, summer,  
506 winter air temperatures accounted for 56%, 28%, and 68% of mass balance variability,  
507 respectively. Of the seasonal air temperatures, winter is more important. The time series of the  
508 contribution to the total mass balance departure was smoothed with a 5-year running mean  
509 and show that winter precipitation and winter air temperature vary most (Figure 8b). The mid-  
510 century cool period ~1946-1977 shows two episodes of cool winter air temperatures (positive  
511 departures of mass balance) simultaneously with two episodes of positive precipitation  
512 departures. The two episodes are separated by a warm winter period (negative mass balance  
513 departures) and average winter precipitation.

514  
515 To examine the influence of broader climate patterns, monthly values of mass balance, air  
516 temperature, and precipitation were smoothed with a 12-month central running mean and  
517 correlated with the climate indices (Table A3). The highest correlations were found between  
518 the PDO, PNA, and NP with monthly air temperatures ( $R^2 = +0.53, +0.64, -0.58$  respectively) and  
519 with mass balance ( $-0.52, -0.59, -0.56$  respectively). Note that PDO, PNA, and NP are highly  
520 inter-correlated (e.g. PDO-PNA,  $+0.66$ ; PNA-NP,  $-0.71$ ) as are air temperature and mass balance  
521 ( $-0.74$ ). Lesser correlations were found with Nino 3.4 and SOI for temperature ( $+0.52, -0.47$ ),  
522 and for mass balance ( $-0.43, +0.40$ ). Correlations between precipitation and the indices did not  
523 exceed  $\pm 0.19$  and the correlation between air temperature and precipitation was also low, -  
524 0.12. Therefore, at annual time scales, PDO, PNA, and NP are the most influential atmospheric  
525 patterns on air temperature and mass balance.

526  
527 The shifts in the mass balance of Blue Glacier coincide with regime shifts of sea surface  
528 temperatures in the North Pacific Ocean, which are typically related to the Pacific Decadal  
529 Oscillation PDO. Shifts occur in 1923, 1946, 1977, and 1998 (Figure 8) (Bond, 2003; Gedalof &  
530 Smith, 2001; Jo et al., 2015; Litzow & Mueter, 2014; Mantua & Hare, 2002; Minobe, 2002;  
531 Overland et al., 2008), and 1998 (Hare & Mantua, 2000; Jo et al., 2015; Minobe, 2002). No clear  
532 response is observed with the 1989 shift suggested by (Hare & Mantua, 2000). The periods of

533 glacier stability, 1890-1924, and 1947-1976 are associated with “cool” PDO regimes, whereas  
534 periods of glacier recession, 1925-1946, and 1977-1998, are associated with “warm” PDO  
535 regimes (Mantua and Hare, 2002). These data show that the mass balance of Blue Glacier  
536 specifically, and by implication those in the Olympic Mountains, are very sensitive to the sea  
537 temperatures conditions of the North Pacific.

538

## 539 **5. The Glacier Future to 2100**

540

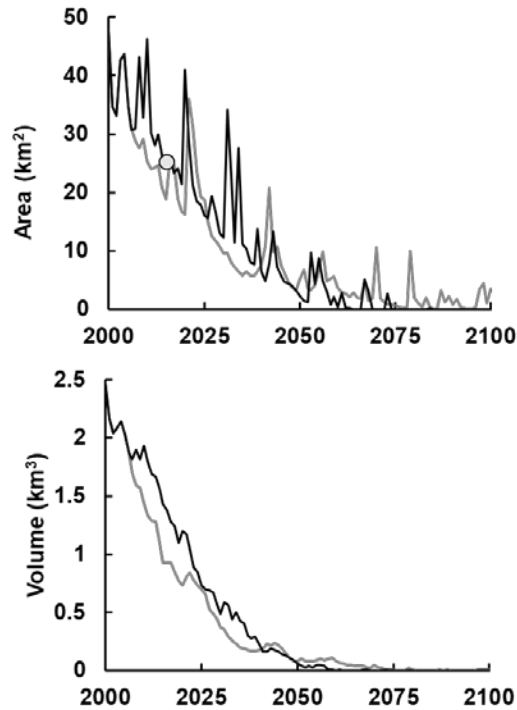
541 To predict the future extent of the glaciers in the Olympic Mountains we applied the Regional  
542 Glaciation Model (RGM) developed by Clarke et al (2015) in modified form. The RGM is a  
543 distributed 2-dimensional, plan-view model. It grows glaciers from a bare-earth landscape at  
544 time steps of one year. The bare-earth landscape at 25m-scale digital elevation model is  
545 estimated by removing the glaciers identified by the Randolph Glacier Inventory using a surface  
546 inversion (Huss & Farinotti, 2012; Pfeffer et al., 2014). The final bare-earth landscape was  
547 rescaled to 100m. To drive the RGM model, monthly meteorological fields from a global climate  
548 model (GCM are downscaled. The Community Climate System Model 4 (CCSM4, Gent et al.,  
549 2011) generated these fields under various emission scenarios for the future. These scenarios  
550 are described as Regional Concentration Pathways (RCP, Van Vuuren et al., 2011) for different  
551 climate scenarios of low ( $2.6 \text{ W m}^{-2}$  of additional forcing by 2100), moderate ( $4.5 \text{ W m}^{-2}$ ), or  
552 “business as usual” ( $8.5 \text{ W m}^{-2}$ ), respectively. The GCM simulations of air temperature,  
553 precipitation, and solar radiation are provided for grid cells  $1^\circ \times 1^\circ$  (latitude, longitude) and one  
554 cell covered the model domain. Spatial variation in air temperature and precipitation across the  
555 model domain was estimated using the Parameter-elevation Relationships on Independent  
556 Slopes Model (PRISM, Daly et al., 2007), an 800 m gridded data set based on weather station  
557 measurements and rescaled to 100m to match the digital elevation model. Monthly PRISM  
558 values, averaged over the period 1980-2010, subtracted from the GCM value, also averaged  
559 over the same period, producing a cell by cell offset for temperature and precipitation (Gray,  
560 2019). We assume the spatial offsets do not change with time. The spatial pattern of solar  
561 radiation is calculated from the solar position at a constant solar angle for that month and the

562 value from the GCM is distributed accordingly. Finally, snow accumulates on the landscape  
563 when precipitation occurs at air temperatures below 0°C. Snow and ice melt are estimated  
564 from a degree-day melt model and exposure to solar radiation.

565  
566 Initial results showed that model could not predict the presence of glaciers in part of the  
567 domain, east of Mount Olympus, despite extreme adjustments to the parameters. We  
568 concluded that the source of the problem was snow accumulation through direct snowfall and  
569 secondary sources of avalanching and wind redistribution. Significant uncertainty plagues  
570 spatially distributed precipitation in mountainous regions (Gutmann et al., 2012; Livneh et al.,  
571 2014). And secondary sources make important contributions to small glaciers (Frans et al.,  
572 2018; Kuhn, 1995). Precipitation was increased by a factor of 3 over the footprint of the glaciers  
573 producing reasonable results for glacier location and extent, similar to the approach of (Clarke  
574 et al., 2015). Results showed the total area of modeled ice in 1980 was 106% of measured and  
575 in 2015, 97%. About 60% of the glaciers were correctly placed. This mismatch is not of great  
576 concern given the coarseness of the model, in terms of spatial resolution and approximation of  
577 the mass balance processes.

578  
579 Over time the model shows a dramatic loss of ice (Figure 11). For the RCP 8.5 “business as  
580 usual” scenario shows that the glaciers will largely vanish by about 2070. With a moderate  
581 reduction in greenhouse gases (RCP 4.5) the total glacier area will be reduced to a few km<sup>2</sup> at  
582 most and limited to Mt. Olympus. The spikey character of the glacier area plot is typical of  
583 widely dispersed small glaciers (Clarke et al., 2015).

584  
585  
586  
587  
588



589

590 *Figure 11. Predicted area and volume for the glaciers of the Olympic Peninsula. The black line is*  
 591 *RCP 8.5 'business as usual' scenario, and the grey line is the RCP 4.5 modest reduction (Van*  
 592 *Vuuren et al., 2011). The dot in the area plot is the measured glacier area in 2015.*

593

## 594 6. DISCUSSION

595

596 Our method of inventorying differed from the original inventory (Spicer, 1989) due to new  
 597 technology and digital imagery. This posed some challenges to developing a seamless series of  
 598 inventories over time. The methodological difference highlighted an important and often  
 599 overlooked issue. When updating an inventory completed by different authors, original  
 600 methods must be understood in order to minimize apparent changes in area resulting from  
 601 methodological differences (Paul et al., 2010; DeVisser and Fountain, 2015; Riedel and  
 602 Larrabee, 2016). This is also true for individual glaciers where interpretations of a glacier  
 603 boundary may differ dramatically between investigators. It is not so much a matter of boundary  
 604 interpretation as assumptions regarding which tributary or connected ice-covered landscape to  
 605 include. Imagery resolution is also important. Our new inventories were compiled from aerial

606 photographs or high-resolution satellite imagery both with a spatial resolution  $\leq 1$  m. This  
607 resolution seemed suitable for outlining small glaciers ( $\geq 0.01$  km<sup>2</sup>) and certainly provides a  
608 much better accuracy than 15 m resolution Landsat (Fischer et al., 2014). Also, compiling  
609 inventories for more than one set of imagery is advantageous because although a single author  
610 may compile the two new inventories some adjustment between inventories is required  
611 because shifting assumptions during the data collection period. A second author compiled the  
612 last inventory and had to reconcile those outlines against the prior two inventories. This  
613 minimized interpretation error over time.

614 The inventories are split into two categories. The partial inventories track only those 261  
615 glaciers  $\geq 0.1$  km<sup>2</sup>, identified in 1980 by Spicer (1986). The complete inventories, starting in  
616 1990, include initially 308 glaciers and perennial snowfields  $\geq 0.01$  km<sup>2</sup>. Although the  
617 inventories differ by 47 features, the total areas did not differ by more than 0.35 km<sup>2</sup> and the  
618 trend with time did not differ. To maintain the longest record the results from the partial  
619 inventories are summarized.

620

621 The Olympic Mountains are populated by small glaciers, as of 2015 the average area was 0.08  
622 km<sup>2</sup>, and they have been shrinking over time like other regions in North America and elsewhere  
623 globally (Abermann et al., 2009; DeBEER & Sharp, 2007; DeVisser & Fountain, 2015). Thirty-five  
624 glaciers and 16 perennial snowfields have disappeared. The pattern of change is also similar  
625 with the smaller glaciers exhibiting a wide range of shrinkage, but generally shrinking faster,  
626 than the larger glaciers, which exhibit a smaller range of shrinkage (Bolch et al., 2010;  
627 Granshaw & Fountain, 2006; Paul, 2004). The total area decreased by -45% since 1980 at a rate  
628 of  $-1.3\%$  yr<sup>-1</sup>, faster than that for western Canada  $-0.6\%$  yr<sup>-1</sup> (1985-2000) (Bolch et al., 2010) and  
629 faster than in the North Cascade Range 100 km to the northeast,  $-0.4\%$  yr<sup>-1</sup> (1959-2009) (Riedel  
630 and Larrabee, 2016). However, as Bolch et al., (2010) point out this difference is probably due  
631 to differences in glacier size because, as a general rule, smaller glaciers retreat faster than  
632 larger glaciers. In addition, the glaciers in the Olympic Mountains are found at lower elevations  
633 than most other regions. The retreat rate in the Olympics is more similar to the retreat rate of  
634 small glaciers in western Canada such as on Vancouver Island ( $-1.11\%$  yr<sup>-1</sup>), the Central Coast (-

635 1.2% yr<sup>-1</sup>), or the Northern Interior (-1.11 % yr<sup>-1</sup>). Our rate is also faster than glaciers in the  
636 Wind River Range, Wyoming, USA (-0.65% yr<sup>-1</sup>, 1966-2006), or the European Alps (-0.9% yr<sup>-1</sup>,  
637 1970 – 2003) although Paul et al. (2011) argue for a rate of about 2% yr<sup>-1</sup> from the mid-1980's  
638 to 2003. In any case, the rate of retreat is within the range of other published studies.

639  
640 Examination of topographic influences on glacier shrinkage showed that elevation was the only  
641 significant influence, similar to other studies (DeVisser & Fountain, 2015). The scatter about the  
642 regression line can be due to any number of factors including glacier hypsometry, aspect, and  
643 slope (Fischer et al., 2015; Tangborn et al., 1990). A confounding factor is that smaller glaciers  
644 generally retreat more than larger glaciers, and the retreat variability is much greater for  
645 smaller glaciers (Figure 4; DeBEER & Sharp, 2007; Granshaw & Fountain, 2006; Paul, 2004). The  
646 presence and change of small glaciers is highly dependent on the interrelation of topographic  
647 and climatic factors (DeBEER & Sharp, 2009; Kessler et al., 2006; Kuhn, 1995). The absence of  
648 hypsometric influence on the magnitude of area change may be due to the relatively small  
649 glaciers that do not span a large elevation range so the climate differs little between the  
650 terminus and head of the glacier.

651  
652 The rate of specific volume changes averaged -0.46 m yr<sup>-1</sup>, 1980-2015, and is comparable to the  
653 mass change of the 30 global reference glaciers for the same time period (WGMS, 2019). Our  
654 value is also close to that for the Olympic Mountains of -0.55 m yr<sup>-1</sup> (2000-2015) estimated from  
655 satellite imagery (Menounos et al., 2018) and to Riedel et al. (2015) of -0.54 m yr<sup>-1</sup> (1980-2009)  
656 based on aerial photographs. Using area-volume scaling, about 0.75 ± 0.19 km<sup>3</sup> of ice remains in  
657 the Olympic Mountains as of 2015. Examining the changes on Mount Olympus, the largest  
658 fraction of glacier-covered area is at 1750 m, but the maximum fractional volume change  
659 (1980-2015) occurs 150 m lower at 1600 m amsl. This is the cross-over point between  
660 decreasing specific volume change with elevation and increasing glacier-covered area. Such an  
661 elevation offset is probably not unusual. Abermann et al. (2009) found similar results in Austria  
662 for area change. Specific volume change no longer decreases with elevation above 2000 m,  
663 becoming constant at -9 m. A similar result, -11 m (1985-1999), occurs for glaciers of British

664 Columbia, Canada (Schiefer et al., 2007). A constant thinning with elevation seems to occur at  
665 about 0.75 of the normalized elevation differences from the terminus to the glacier head in a  
666 number of regions (Arendt et al., 2006; Schiefer et al., 2007). The constant thinning at the  
667 upper-most elevations is similar to the constant mass balance at the upper-most elevations of  
668 individual glaciers and not a unique finding (Dyurgerov et al., 2002). The effect of altitude on  
669 ablation and accumulation can decrease significantly at high elevation due to cooler air  
670 temperatures, snowfall may decrease with elevation due to limits on cloud elevation, and high  
671 winds at elevation redistributes snow erasing an elevation dependence.

672

673 Based on the mass balance model of Blue Glacier, it is clear that variations in mass balance are  
674 highly sensitive to variations in air temperature (83% of the variability) and less so to variations  
675 in precipitation (53%), given their low elevation and high mass turnover. This is a known  
676 attribute of maritime glaciers (Anderson & Mackintosh, 2012; Oerlemans & Fortuin, 1992).

677 Overall the retreat of these glaciers is due to increasing air temperatures over the past century,  
678 which has warmed by almost 1°C in winter, which can change the phase of precipitation from  
679 snow to rain reducing mass accumulation and by about +0.3°C in summer, which increases  
680 melt. The Olympic Mountains have been identified as one of the regions within the Pacific  
681 Northwest with warm snowpacks vulnerable to winter warming and increasing proportions of  
682 winter rain rather than snow (Klos et al., 2014; Nolin & Daly, 2006).

683

684 Of the climate indices correlated with monthly air temperatures and mass balance of Blue  
685 Glacier and therefore the glaciers of the Olympic Mountains, the PNA and PDO patterns were  
686 the strongest. PNA is a measure of the amplitude of the planetary wave field of atmospheric  
687 heights (pressures) over the northeast Pacific and North America at intramonthly time scales. It  
688 is correlated with freezing level in the atmosphere over western North America and most highly  
689 correlated over coastal Oregon and Washington (Abatzoglous, 2011). The PNA documents  
690 changes in atmospheric circulation, which contributes to wintertime warming and has been  
691 shown to correlate with snowpack generally in the western US (Barnston & Livezey, 1987;  
692 Cayan, 1996; Gutzler & Rosen, 1992). The impact of warming winter air temperatures on snow

693 accumulation in the western US has been described generally (McCabe & Wolock, 2009; Mote  
694 et al., 2005, 2018) and specifically for Blue Glacier (Rasmussen & Conway, 2000). Given that the  
695 mass balance of Blue Glacier is highly sensitive to air temperature correlation with the PNA  
696 index is not surprising. For PDO, the statistically significant correlation between temperature  
697 and mass balance is also reflective of conditions in the North Pacific. The PDO, based on sea  
698 surface temperatures, tends to vary over decadal time scales and is highly correlated with the  
699 PNA (Mantua and Hare, 2002; Newman et al., 2016). Like the PNA, the PDO is also correlated  
700 with snowpack variability such that positive PDO values, indicate warming along the coast of  
701 the Pacific Northwest and warmer air temperatures and reduced snow accumulation in the  
702 Pacific Northwest (McCabe & Dettinger, 2002; Zhang et al., 2010). It is striking that the shifts in  
703 the trend of mass balance of Blue Glacier are highly correlated with changes in the state of the  
704 Pacific Ocean, which is related to the PDO. They also largely explain the variation in winter mass  
705 accumulation estimated by Rasmussen & Conway (2000). The ‘warm’ phases of the PDO, where  
706 the ocean waters along the coast of western North America are warmer than normal, coincide  
707 with periods of decreasing mass balance whereas ‘cool’ phases are associated with the glacier  
708 mass balance in equilibrium or slightly gaining. This relationship has also been noted for Blue  
709 Glacier by Malcomb and Wiles (2013).

710

711 The response of glacier mass balance to climate indices in the Pacific Northwest have been well  
712 explored and show that the glacier mass balance is sensitive to conditions in the North Pacific  
713 Ocean (Bitz & Battisti, 1999; Hodge et al., 1998; Walters & Meier, 1989). Using the measured  
714 mass balance record from South Cascade Glacier, 150 km to the northeast of Blue Glacier in the  
715 Cascade Mountains, McCabe and Fountain (1995) showed that variations in in annual mass  
716 balance were driven by winter snow accumulation. From that Hodge et al., (1998) showed good  
717 correlations between winter mass balance and PNA; Bitz and Battisti (1999) showed good  
718 correlations with PDO and much less so with ENSO. McCabe and Fountain (1995) examined the  
719 correlations between the 700 mb atmospheric pressure field and the winter mass balance,  
720 finding a correlative pressure pattern across western North America similar to the PNA.  
721 Atmospheric circulation patterns that increase zonal westerly flow from the Pacific Ocean to

722 the Pacific Northwest have been shown to increase precipitation, particularly in high alpine  
723 terrain (Luce et al., 2013; Menounos et al., 2018; Shea & Marshall, 2007). Increases in such  
724 precipitation in winter, if air temperatures are below freezing, increase glacier mass balance.  
725 However, increasingly warm winter climate since 2000 suggests that the cool phase of the PDO  
726 is also becoming warmer reducing its ability to nourish the glaciers (Josberger et al., 2007).

727

728 The predicted demise of the glaciers by 2100 is not unique. Predictions of glacier change in  
729 western Canada suggest a 70% volume loss by 2100 but for the Coastal Mountains of the  
730 Central Coast and Vancouver Island, complete loss on or before 2100 (Clarke et al., 2015) (see  
731 also supplementary material). This supports prior work in along the eastern slopes of the  
732 Canadian Rocky Mountains and for selected glacier-populated basins in the Pacific Northwest  
733 that are predicted to lose 80-90% of the glacier volume by 2100 (Frans et al., 2018; Marshall et  
734 al., 2011). Predictions of global alpine glacier change suggest rapid loss for the rest of the  
735 century and for the region of western Canada and US, exclusive of Alaska, at least 50% loss  
736 (Radić & Hock, 2011).

737

## 738 **7. Conclusions**

739

740 Careful updating of prior glacier inventories is required to avoid introducing error based on  
741 methodological differences or different assumptions regarding glacier boundaries. Glacier by  
742 glacier comparisons between inventories minimized such errors.

743 The initial inventory of glaciers in the Olympic Mountains showed that the total area in 1980  
744 was  $45.9 \pm 0.51 \text{ km}^2$  with a mean glacier area of  $0.18 \text{ km}^2$ . By 2015 the total area decreased  $-45$   
745  $\pm 0.02 \%$ , mean glacier area decreased to  $0.08 \text{ km}^2$ , and 35 glaciers and 16 perennial snowfields  
746 disappeared. Over this period glacier area decreased at a rate of  $-0.59 \text{ km}^2 \text{ yr}^{-1}$ , with the fastest  
747 rate during the 2009-2015 period,  $-0.82 \pm 0.02 \text{ km}^2 \text{ yr}^{-1}$ . Like other studies elsewhere, smaller  
748 glaciers retreated more than larger glaciers, they also showed the most variability. The  
749 variability is probably a result of favorable local conditions that decrease melt and increase  
750 accumulation compared to less favorable conditions. To infer changes prior to 1980 we used

751 Blue Glacier, the largest ( $5.143 \pm 0.094 \text{ km}^2$  in 2015) and most well documented glacier in the  
752 region, as a proxy for regional glacier change because of its high correlation with the regional  
753 area change. In 1900, the total area covered by glaciers was  $55.3 \text{ km}^2$  more than twice the area  
754 in 2015.

755 A simple mass balance model of Blue Glacier, based on monthly air temperature and  
756 precipitation, showed good correspondence with changes in glacier area. Interrogation of the  
757 model showed that variations in monthly mass accumulation is better explained by variations in  
758 air temperature than precipitation, suggesting the importance of temperature control on the  
759 precipitation phase. Ablation is highly correlated with temperature alone. Taken together air  
760 temperature is the dominant influence on glacier mass balance in the Olympic Mountains,  
761 explaining 83% of the variance, with precipitation playing a secondary role. This is common to  
762 glaciers in maritime climates where winter air temperatures are close to the  $0^\circ\text{C}$  threshold and  
763 only a small change in temperature can change the phase of the precipitation from snow to  
764 rain. The mass changes are highly correlated with the Pacific North American index, a measure  
765 of the strength of zonal versus meridional air flow over North America at weekly-seasonal time  
766 scales. The changes are also correlated with regime shifts of the Pacific Decadal Oscillation, a  
767 measure of sea surface temperatures in the North Pacific that varies over decadal time scales.  
768 Finally, the future of these glaciers is grim. Using a coupled global circulation model with a  
769 distributed glacier flow model shows that the glaciers of the Olympic Mountains should largely  
770 disappear by 2070.

## 771 **Acknowledgements**

772 Supplementary Online Data can be found at, <https://doi.org/10.15760/geology-data.02> The  
773 authors wish to acknowledge Steve Wilson who collected some of the early data and to Greg  
774 McCabe who provided very helpful comments on the climate section. This work was funded by  
775 the US Geological Survey via the Western Mountain Initiative.

776

## 777 **Author Contributions**

778 Andrew G. Fountain identified the goals and aims of the project, and participating in all phases  
779 of analysis and wrote the paper. Christina Gray applied the regional glaciation model to the

780 Olympic Mountains and edited the paper. Bryce Glenn created the 2015 glacier inventory and  
781 did the GIS analysis of glacier change, topography and climate across the region. Brian  
782 Menounos adapted the original formulation of regional glaciation model to include paleo GCM  
783 input, helped with preparing datasets for model inclusion, advised Christina on model  
784 implementation, and helped with the editing. Justin Pflug supplied the 2015 DEM data used for  
785 estimating glacier volume change and helped edit the paper. Jon Riedel supplied some of the  
786 glacier area data prior to 2015 and helped edit the paper.

787

788

789 **References**

- 790
- 791 Abermann, J., Lambrecht, A., Fischer, A., & Kuhn, M. (2009). Quantifying changes and trends in  
792 glacier area and volume in the Austrian Ötztal Alps (1969–1997–2006). *The Cryosphere*  
793 *Discussions*, 3(2), 415–441. <https://doi.org/10.5194/tc-3-205-2009>
- 794 Abatzoglou, J. T. (2011). Influence of the PNA on declining mountain snowpack in the Western  
795 United States. *International Journal of Climatology*, 31(8), 1135–1142.  
796 <https://doi.org/10.1002/joc.2137>
- 797 AGS. (1960). *Nine Glacier Maps, Northwestern North America: Accompanied by Nine Separate*  
798 *Map Sheets on Scale of 1: 10,000*. American Geographical Society, Vol. 34, Lane Press.
- 799 Anderson, B., & Mackintosh, A. (2012). Controls on mass balance sensitivity of maritime glaciers  
800 in the Southern Alps, New Zealand: The role of debris cover. *Journal of Geophysical*  
801 *Research*, 117(F1). <https://doi.org/10.1029/2011JF002064>
- 802 Arendt, A., Echelmeyer, K., Harrison, W., Lingle, C., Zirnheld, S., Valentine, V., Ritchie, B., &  
803 Druckenmiller, M. (2006). Updated estimates of glacier volume changes in the western  
804 Chugach Mountains, Alaska, and a comparison of regional extrapolation methods.  
805 *Journal of Geophysical Research*, 111(F3). <https://doi.org/10.1029/2005JF000436>
- 806 Armstrong, R. L. (1989). Mass balance history of Blue Glacier, Washington, USA. In J. Oerlemans  
807 (Ed.), *Glacier Fluctuations and Climatic Change* (pp. 183–192). Springer Netherlands.
- 808 Bahr, D. B., Pfeffer, W. T., & Kaser, G. (2015). A review of volume-area scaling of glaciers:  
809 Volume-Area Scaling. *Reviews of Geophysics*, 53(1), 95–140.  
810 <https://doi.org/10.1002/2014RG000470>

811 Baird, D. C. (1962). *Experimentation: An introduction to measurement theory and experiment*  
812 *design*. Prentice Hall. <https://doi.org/0-13-295345-5>

813 Barnston, A. G., & Livezey, R. E. (1987). Classification, seasonality and persistence of low-  
814 frequency atmospheric circulation patterns. *Monthly Weather Review*, *115*(6), 1083–  
815 1126. [https://doi.org/10.1175/1520-0493\(1987\)115<1083:CSAPOL>2.0.CO;2](https://doi.org/10.1175/1520-0493(1987)115<1083:CSAPOL>2.0.CO;2)

816 Basagic, H. J., & Fountain, A. G. (2011). Quantifying 20th Century Glacier Change in the Sierra  
817 Nevada, California. *Arctic, Antarctic, and Alpine Research*, *43*(3), 317–330.  
818 <https://doi.org/10.1657/1938-4246-43.3.317>

819 Bitz, C. M., & Battisti, D. S. (1999). Interannual to Decadal Variability in Climate and the Glacier  
820 Mass Balance in Washington, Western Canada, and Alaska. *Journal of Climate*, *12*(11),  
821 3181–3196. [https://doi.org/10.1175/1520-0442\(1999\)012<3181:ITDVIC>2.0.CO;2](https://doi.org/10.1175/1520-0442(1999)012<3181:ITDVIC>2.0.CO;2)

822 Bjerknes, J. (1966). A possible response of the atmospheric Hadley circulation to equatorial  
823 anomalies of ocean temperature. *Tellus*, *18*(4), 820–829.  
824 <https://doi.org/10.3402/tellusa.v18i4.9712>

825 Bolch, T., Menounos, B., & Wheate, R. (2010). Landsat-based inventory of glaciers in western  
826 Canada, 1985–2005. *Remote Sensing of Environment*, *114*(1), 127–137.  
827 <https://doi.org/10.1016/j.rse.2009.08.015>

828 Bond, N. A. (2003). Recent shifts in the state of the North Pacific. *Geophysical Research Letters*,  
829 *30*(23). <https://doi.org/10.1029/2003GL018597>

830 Cayan, D. R. (1996). Interannual Climate Variability and Snowpack in the Western United States.  
831 *Journal of Climate*, *9*(5), 928–948. [https://doi.org/10.1175/1520-](https://doi.org/10.1175/1520-0442(1996)009<0928:ICVASI>2.0.CO;2)  
832 [0442\(1996\)009<0928:ICVASI>2.0.CO;2](https://doi.org/10.1175/1520-0442(1996)009<0928:ICVASI>2.0.CO;2)

833 Chen, J., & Ohmura, A. (1990). Estimation of Alpine glacier water resources and their change  
834 since the 1870s. *IAHS Publ*, 193, 127–135.

835 Chen, W. (1982). Assessment of Southern Oscillation sea-level pressure indices. *Monthly*  
836 *Weather Review*, 110(7), 800–807. [https://doi.org/10.1175/1520-](https://doi.org/10.1175/1520-0493(1982)110<0800:AOSOSL>2.0.CO;2)  
837 [0493\(1982\)110<0800:AOSOSL>2.0.CO;2](https://doi.org/10.1175/1520-0493(1982)110<0800:AOSOSL>2.0.CO;2)

838 Clarke, G. K. C., Jarosch, A. H., Anslow, F. S., Radić, V., & Menounos, B. (2015). Projected  
839 deglaciation of western Canada in the twenty-first century. *Nature Geoscience*.  
840 <https://doi.org/10.1038/ngeo2407>

841 Clow, D. W., & Sueker, J. K. (2000). Relations between basin characteristics and stream water  
842 chemistry in alpine/subalpine basins in Rocky Mountain National Park, Colorado. *Water*  
843 *Resources Research*, 36(1), 49–61. <https://doi.org/10.1029/1999WR900294>

844 Conway, H., Rasmussen, L. A., & Marshall, H. P. (1999). Annual mass balance of Blue Glacier,  
845 USA: 1955-97. *Geografiska Annaler: Series A, Physical Geography*, 81(4), 509–520.  
846 <https://doi.org/10.1111/1468-0459.00080>

847 Cuffey, K. M., & Paterson, W. S. B. (2010). *The Physics of Glaciers* (4th ed.). Academic Press.

848 Daly, C., Smith, J. W., Smith, J. I., & McKane, R. B. (2007). High-Resolution Spatial Modeling of  
849 Daily Weather Elements for a Catchment in the Oregon Cascade Mountains, United  
850 States. *Journal of Applied Meteorology and Climatology*, 46(10), 1565–1586.  
851 <https://doi.org/10.1175/JAM2548.1>

852 DeBEER, C. M., & Sharp, M. J. (2007). Recent changes in glacier area and volume within the  
853 southern Canadian Cordillera. *Annals of Glaciology*, 46(1), 215–221.  
854 <https://doi.org/10.3189/172756407782871710>

855 DeBEER, C. M., & Sharp, M. J. (2009). Topographic influences on recent changes of very small  
856 glaciers in the Monashee Mountains, British Columbia, Canada. *Journal of Glaciology*,  
857 55(192), 691–700. <https://doi.org/10.3189/002214309789470851>

858 DeVisser, M. H., & Fountain, A. G. (2015). A century of glacier change in the Wind River Range,  
859 WY. *Geomorphology*, 232, 103–116. <https://doi.org/10.1016/j.geomorph.2014.10.017>

860 Dyurgerov, M., Meier, M., & Armstrong, R. L. (2002). *Glacier mass balance and regime: Data of*  
861 *measurements and analysis*. Institute of Arctic and Alpine Research, University of  
862 Colorado Boulder,, USA.  
863 [ftp://sidads.colorado.edu/DATASETS/NOAA/G10002/Occasional\\_Paper55/instaar\\_occasional\\_paper\\_no55.pdf](ftp://sidads.colorado.edu/DATASETS/NOAA/G10002/Occasional_Paper55/instaar_occasional_paper_no55.pdf)

865 Elder, K., Dozier, J., & Michaelsen, J. (1991). Snow accumulation and distribution in an alpine  
866 watershed. *Water Resources Research*, 27(7), 1541–1552.  
867 <https://doi.org/10.1029/91WR00506>

868 Farinotti, D., Huss, M., Bauder, A., Funk, M., & Truffer, M. (2009). A method to estimate the ice  
869 volume and ice-thickness distribution of alpine glaciers. *Journal of Glaciology*, 55(191),  
870 422–430. <https://doi.org/10.3189/002214309788816759>

871 Fischer, M., Huss, M., & Hoelzle, M. (2015). Surface elevation and mass changes of all Swiss  
872 glaciers 1980–2010. *The Cryosphere*, 9(2), 525–540. [https://doi.org/10.5194/tc-9-525-](https://doi.org/10.5194/tc-9-525-2015)  
873 2015

874 Fischer, Mauro, Huss, M., Barboux, C., & Hoelzle, M. (2014). The New Swiss Glacier Inventory  
875 SGI2010: Relevance of Using High-Resolution Source Data in Areas Dominated by Very

876 Small Glaciers. *Arctic, Antarctic, and Alpine Research*, 46(4), 933–945.  
877 <https://doi.org/10.1657/1938-4246-46.4.933>

878 Fountain, A. G., Glenn, B., & Basagic, H. J. (2017). The Geography of Glaciers and Perennial  
879 Snowfields in the American West. *Arctic, Antarctic, and Alpine Research*, 49(3), 391–410.  
880 <https://doi.org/10.1657/AAAR0017-003>

881 Fountain, A. G., Hoffman, M. J., Jackson, K., Basagic, H. J., Nylén, T. H., & Percy, D. (2007).  
882 *Digital outlines and the topography of the Glaciers of the American West* (Open File  
883 Report No. 2006–1340; p. 23). US Geological Survey.  
884 <https://doi.org/10.3133/ofr20061340>

885 Frans, C., Istanbuluoglu, E., Lettenmaier, D. P., Fountain, A. G., & Riedel, J. (2018). Glacier  
886 Recession and the Response of Summer Streamflow in the Pacific Northwest United  
887 States, 1960-2099. *Water Resources Research*. <https://doi.org/10.1029/2017WR021764>

888 Gedalof, Z., & Smith, D. J. (2001). Interdecadal climate variability and regime-scale shifts in  
889 Pacific North America. *Geophysical Research Letters*, 28(8), 1515–1518.  
890 <https://doi.org/10.1029/2000GL011779>

891 Gent, P. R., Danabasoglu, G., Donner, L. J., Holland, M. M., Hunke, E. C., Jayne, S. R., Lawrence,  
892 D. M., Neale, R. B., Rasch, P. J., & Vertenstein, M. (2011). The community climate system  
893 model version 4. *Journal of Climate*, 24(19), 4973–4991.  
894 <https://doi.org/10.1175/2011JCLI4083.1>

895 Gesch, D., Oimoen, M., Greenlee, S., Nelson, C., Steuck, M., & Tyler, D. (2002). The national  
896 elevation dataset. *Photogrammetric Engineering and Remote Sensing*, 68(1), 5–32.

897 Ghilani, C. D. (2000). Demystifying area uncertainty: More or less. *Surveying and Land*  
898 *Information Systems*, 60(3), 177–182.

899 Gorelick, N., Hancher, M., Dixon, M., Ilyushchenko, S., Thau, D., & Moore, R. (2017). Google  
900 Earth Engine: Planetary-scale geospatial analysis for everyone. *Remote Sensing of*  
901 *Environment*, 202, 18–27. <https://doi.org/10.1016/j.rse.2017.06.031>

902 Granshaw, F. D., & Fountain, A. G. (2006). Glacier change (1958–1998) in the North Cascades  
903 National Park Complex, Washington, USA. *Journal of Glaciology*, 52(177), 251–256.  
904 <https://doi.org/10.3189/172756506781828782>

905 Gutmann, E. D., Rasmussen, R. M., Liu, C., Ikeda, K., Gochis, D. J., Clark, M. P., Dudhia, J., &  
906 Thompson, G. (2012). A comparison of statistical and dynamical downscaling of winter  
907 precipitation over complex terrain. *Journal of Climate*, 25(1), 262–281.  
908 <https://doi.org/10.1175/2011JCLI4109.1>

909 Gutzler, D. S., & Rosen, R. D. (1992). Interannual Variability of Wintertime Snow Cover across  
910 the Northern Hemisphere. *Journal of Climate*, 5(12), 1441–1447.  
911 [https://doi.org/10.1175/1520-0442\(1992\)005<1441:IVOWSC>2.0.CO;2](https://doi.org/10.1175/1520-0442(1992)005<1441:IVOWSC>2.0.CO;2)

912 Hare, S. R., & Mantua, N. J. (2000). Empirical evidence for North Pacific regime shifts in 1977  
913 and 1989. *Progress in Oceanography*, 47(2–4), 103–145. [https://doi.org/10.1016/S0079-](https://doi.org/10.1016/S0079-6611(00)00033-1)  
914 [6611\(00\)00033-1](https://doi.org/10.1016/S0079-6611(00)00033-1)

915 Hodge, S. M., Trabant, D. C., Krimmel, R. M., Heinrichs, T. A., March, R. S., & Josberger, E. G.  
916 (1998). Climate variations and changes in mass of three glaciers in western North  
917 America. *Journal of Climate*, 11(9), 2161–2179. [https://doi.org/10.1175/1520-](https://doi.org/10.1175/1520-0442(1998)011<2161:CVACIM>2.0.CO;2)  
918 [0442\(1998\)011<2161:CVACIM>2.0.CO;2](https://doi.org/10.1175/1520-0442(1998)011<2161:CVACIM>2.0.CO;2)

919 Hoffman, M. J., Fountain, A. G., & Achuff, J. M. (2007). 20th-century variations in area of cirque  
920 glaciers and glacierets, Rocky Mountain National Park, Rocky Mountains, Colorado, USA.  
921 *Annals of Glaciology*, 46(1), 349–354. <https://doi.org/10.3189/172756407782871233>

922 Huss, M., & Farinotti, D. (2012). Distributed ice thickness and volume of all glaciers around the  
923 globe. *Journal of Geophysical Research*, 117(F4). <https://doi.org/10.1029/2012JF002523>

924 Jiskoot, H., Curran, C. J., Tessler, D. L., & Shenton, L. R. (2009). Changes in Clemenceau Icefield  
925 and Chaba Group glaciers, Canada, related to hypsometry, tributary detachment,  
926 length–slope and area–aspect relations. *Annals of Glaciology*, 50(53), 133–143. ).  
927 <https://doi.org/10.3189/172756410790595796>

928 Jo, H.-S., Yeh, S.-W., & Lee, S.-K. (2015). Changes in the relationship in the SST variability  
929 between the tropical Pacific and the North Pacific across the 1998/1999 regime shift.  
930 *Geophysical Research Letters*, 42(17), 7171–7178.  
931 <https://doi.org/10.1002/2015GL065049>

932 Jones, P. D., Jonsson, T., & Wheeler, D. (1997). Extension to the North Atlantic Oscillation using  
933 early instrumental pressure observations from Gibraltar and South-west Iceland.  
934 *International Journal of Climatology*, 17, 1433–1450.  
935 [https://doi.org/10.1002/\(SICI\)1097-0088\(19971115\)17:13<1433::AID-JOC203>3.0.CO;2-](https://doi.org/10.1002/(SICI)1097-0088(19971115)17:13<1433::AID-JOC203>3.0.CO;2-P)  
936 P

937 Josberger, E. G., Bidlake, W. R., March, R. S., & Kennedy, B. W. (2007). Glacier mass-balance  
938 fluctuations in the Pacific Northwest and Alaska, USA. *Annals of Glaciology*, 46, 291–  
939 296. <https://doi.org/10.3189/172756407782871314>

940 Kessler, M. A., Anderson, R. S., & Stock, G. M. (2006). Modeling topographic and climatic  
941 control of east-west asymmetry in Sierra Nevada glacier length during the Last Glacial  
942 Maximum. *Journal of Geophysical Research*, 111(F2).  
943 <https://doi.org/10.1029/2005JF000365>

944 Klos, P. Z., Link, T. E., & Abatzoglou, J. T. (2014). Extent of the rain-snow transition zone in the  
945 western U.S. under historic and projected climate: Climatic rain-snow transition zone.  
946 *Geophysical Research Letters*, 41(13), 4560–4568.  
947 <https://doi.org/10.1002/2014GL060500>

948 Kuhn, M. (1995). The mass balance of very small glaciers. *Zeitschrift Fur Gletscherkunde Und*  
949 *Glazialgeologie*, 5, 171–179.

950 LaChapelle, E. (1959). Annual mass and energy exchange on the Blue Glacier. *Journal of*  
951 *Geophysical Research*, 64(4), 443–449. <https://doi.org/10.1029/JZ064i004p00443>

952 LaChapelle, Edward. (1965). Mass Budget of Blue Glacier, Washington. *Journal of Glaciology*,  
953 5(41), 609–623. <https://doi.org/10.3189/S0022143000018633>

954 Litzow, M. A., & Mueter, F. J. (2014). Assessing the ecological importance of climate regime  
955 shifts: An approach from the North Pacific Ocean. *Progress in Oceanography*, 120, 110–  
956 119. <https://doi.org/10.1016/j.pocean.2013.08.003>

957 Livneh, B., Deems, J. S., Schneider, D., Barsugli, J. J., & Molotch, N. P. (2014). Filling in the gaps:  
958 Inferring spatially distributed precipitation from gauge observations over complex  
959 terrain. *Water Resources Research*, 50(11), 8589–8610.  
960 <https://doi.org/10.1002/2014WR015442>

961 Luce, C. H., Abatzoglou, J. T., & Holden, Z. A. (2013). The Missing Mountain Water: Slower  
962 Westerlies Decrease Orographic Enhancement in the Pacific Northwest USA. *Science*,  
963 342(6164), 1360–1364. <https://doi.org/10.1126/science.1242335>

964 Malcomb, N. L., & Wiles, G. C. (2013). Tree-ring-based reconstructions of North American  
965 glacier mass balance through the Little Ice Age—Contemporary warming transition.  
966 *Quaternary Research*, 79(2), 123–137. <https://doi.org/10.1016/j.yqres.2012.11.005>

967 Mantua, N. J., & Hare, S. R. (2002). The Pacific decadal oscillation. *Journal of Oceanography*,  
968 58(1), 35–44. <https://doi.org/10.1023/A:1015820616384>

969 Marshall, S. J., White, E. C., Demuth, M. N., Bolch, T., Wheate, R., Menounos, B., Beedle, M. J.,  
970 & Shea, J. M. (2011). Glacier Water Resources on the Eastern Slopes of the Canadian  
971 Rocky Mountains. *Canadian Water Resources Journal*, 36(2), 109–134.  
972 <https://doi.org/10.4296/cwrj3602823>

973 McCabe, G. J., & Dettinger, M. D. (2002). Primary modes and predictability of year-to-year  
974 snowpack variations in the western United States from teleconnections with Pacific  
975 Ocean climate. *Journal of Hydrometeorology*, 3(1), 13–25.  
976 [https://doi.org/10.1175/1525-7541\(2002\)003<0013:PMAPOY>2.0.CO;2](https://doi.org/10.1175/1525-7541(2002)003<0013:PMAPOY>2.0.CO;2)

977 McCabe, G. J., & Fountain, A. G. (1995). Relations between atmospheric circulation and mass  
978 balance of South Cascade Glacier, Washington, USA. *Arctic and Alpine Research*, 27(3),  
979 226–233. <https://doi.org/10.1080/00040851.1995.12003117>

980 McCabe, G. J., & Fountain, A. G. (2013). Glacier variability in the conterminous United States  
981 during the twentieth century. *Climatic Change*, 116(3–4), 565–577.  
982 <https://doi.org/10.1007/s10584-012-0502-9>

983 McCabe, G. J., & Wolock, D. M. (2009). Recent Declines in Western U.S. Snowpack in the  
984 Context of Twentieth-Century Climate Variability. *Earth Interactions*, 13(12), 1–15.  
985 <https://doi.org/10.1175/2009EI283.1>

986 Menounos, B., Hugonnet, R., Shean, D., Gardner, A., Howat, I., Berthier, E., Pelto, B., Tennant,  
987 C., Shea, J., Noh, M., Brun, F., & Dehecq, A. (2018). Heterogeneous changes in western  
988 North American glaciers linked to decadal variability in zonal wind strength. *Geophysical*  
989 *Research Letters*. <https://doi.org/10.1029/2018GL080942>

990 Minobe, S. (2002). Interannual to interdecadal changes in the Bering Sea and concurrent  
991 1998/99 changes over the North Pacific. *Progress in Oceanography*, 55(1–2), 45–64.  
992 [https://doi.org/10.1016/S0079-6611\(02\)00069-1](https://doi.org/10.1016/S0079-6611(02)00069-1)

993 Mote, P. W., Hamlet, A. F., Clark, M. P., & Lettenmaier, D. P. (2005). Declining mountain  
994 snowpack in western North America. *Bulletin of the American Meteorological Society*,  
995 86(1), 39–49. <https://doi.org/10.1175/BAMS-86-1-39>

996 Mote, P. W., Li, S., Lettenmaier, D. P., Xiao, M., & Engel, R. (2018). Dramatic declines in  
997 snowpack in the western US. *Climate and Atmospheric Science*, 1(1).  
998 <https://doi.org/10.1038/s41612-018-0012-1>

999 Newman, M., Alexander, M. A., Ault, T. R., Cobb, K. M., Deser, C., Di Lorenzo, E., Mantua, N. J.,  
1000 Miller, A. J., Minobe, S., & Nakamura, H. (2016). The Pacific decadal oscillation, revisited.  
1001 *Journal of Climate*, 29(12), 4399–4427. <https://doi.org/10.1175/JCLI-D-15-0508.1>

1002 NOAA (2018). [www.esrl.noaa.gov/psd/gcos\\_wgsp/Timeseries/](http://www.esrl.noaa.gov/psd/gcos_wgsp/Timeseries/) Accessed, August 2018

1003 Nolin, A. W., & Daly, C. (2006). Mapping “at risk” snow in the Pacific Northwest. *Journal of*  
1004 *Hydrometeorology*, 7(5), 1164–1171. <https://doi.org/10.1175/JHM543.1>

1005 Oerlemans, J., & Fortuin, J. (1992). Sensitivity of glaciers and small ice caps to greenhouse  
1006 warming. *Science*, 258(5079), 115–117. <https://doi.org/10.1126/science.258.5079.115>

1007 OSU, 2017. [www.prism.oregonstate.edu](http://www.prism.oregonstate.edu), accessed November 2017.

1008 Overland, J., Rodionov, S., Minobe, S., & Bond, N. (2008). North Pacific regime shifts:  
1009 Definitions, issues and recent transitions. *Progress in Oceanography*, 77(2–3), 92–102.  
1010 <https://doi.org/10.1016/j.pocean.2008.03.016>

1011 Painter, T. H., Berisford, D. F., Boardman, J. W., Bormann, K. J., Deems, J. S., Gehrke, F., Hedrick,  
1012 A., Joyce, M., Laidlaw, R., Marks, D., Mattmann, C., McGurk, B., Ramirez, P., Richardson,  
1013 M., Skiles, S. M., Seidel, F. C., & Winstral, A. (2016). The Airborne Snow Observatory:  
1014 Fusion of scanning lidar, imaging spectrometer, and physically-based modeling for  
1015 mapping snow water equivalent and snow albedo. *Remote Sensing of Environment*, 184,  
1016 139–152. <https://doi.org/10.1016/j.rse.2016.06.018>

1017 Paul, F., Frey, H., & Le Bris, R. (2011). A new glacier inventory for the European Alps from  
1018 Landsat TM scenes of 2003: Challenges and results. *Annals of Glaciology*, 52(59), 144–  
1019 152. <https://doi.org/10.3189/172756411799096295>

1020 Paul, F. (2004). Rapid disintegration of Alpine glaciers observed with satellite data. *Geophysical*  
1021 *Research Letters*, 31(21). <https://doi.org/10.1029/2004GL020816>

1022 Paul, F., Barry, R. G., Cogley, J. G., Frey, H., Haeberli, W., Ohmura, A., Ommney, C. S. L., Raup,  
1023 B., Rivera, A., & Zemp, M. (2010). Guidelines for the compilation of glacier inventory  
1024 data from digital sources. *Annals of Glaciology*, 50(53), 119–126.  
1025 <https://doi.org/10.3189/172756410790595778>

- 1026 Pfeffer, W. T., Arendt, A. A., Bliss, A., Bolch, T., Cogley, J. G., Gardner, A. S., Hagen, J.-O., Hock,  
1027 R., Kaser, G., & Kienholz, C. (2014). The Randolph Glacier Inventory: A globally complete  
1028 inventory of glaciers. *Journal of Glaciology*, 60(221), 537–552.  
1029 <https://doi.org/10.3189/2014JoG13J176>
- 1030 Radić, V., & Hock, R. (2011). Regionally differentiated contribution of mountain glaciers and ice  
1031 caps to future sea-level rise. *Nature Geoscience*, 4(2), 91–94.  
1032 <https://doi.org/10.1038/ngeo1052>
- 1033 Rasmussen, L. A., Conway, H., & Hayes, P. S. (2000). The accumulation regime of Blue Glacier,  
1034 USA, 1914–96. *Journal of Glaciology*, 46(153), 326–334.  
1035 <https://doi.org/10.3189/172756500781832846>
- 1036 Rayner, N., Parker, D. E., Horton, E., Folland, C., Alexander, L., Rowell, D., Kent, E., & Kaplan, A.  
1037 (2003). Global analyses of sea surface temperature, sea ice, and night marine air  
1038 temperature since the late nineteenth century. *Journal of Geophysical Research:*  
1039 *Atmospheres*, 108(D14), 2156–2202. <https://doi.org/10.1029/2002JD002670>
- 1040 Riedel, Jon L., & Larrabee, M. A. (2016). Impact of Recent Glacial Recession on Summer  
1041 Streamflow in the Skagit River. *Northwest Science*, 90(1), 5–22.  
1042 <https://doi.org/10.3955/046.090.0103>
- 1043 Riedel, Jon L., Wilson, S., Baccus, W., Larrabee, M., Fudge, T. J., & Fountain, A. (2015). Glacier  
1044 status and contribution to streamflow in the Olympic Mountains, Washington, USA.  
1045 *Journal of Glaciology*, 61(225), 8–16. <https://doi.org/10.3189/2015JoG14J138>

- 1046 Riedel, Jon L., & Larrabee, M. A. (2016). Impact of Recent Glacial Recession on Summer  
1047 Streamflow in the Skagit River. *Northwest Science*, *90*(1), 5–22.  
1048 <https://doi.org/10.3955/046.090.0103>
- 1049 Ropelewski, C. F., & Jones, P. D. (1987). An extension of the Tahiti–Darwin southern oscillation  
1050 index. *Monthly Weather Review*, *115*(9), 2161–2165.
- 1051 Schiefer, E., Menounos, B., & Wheate, R. (2007). Recent volume loss of British Columbian  
1052 glaciers, Canada: Volume loss of BC glaciers. *Geophysical Research Letters*, *34*(16),  
1053 L16503. <https://doi.org/10.1029/2007GL030780>
- 1054 Shea, J. M., & Marshall, S. J. (2007). Atmospheric flow indices, regional climate, and Glacier  
1055 mass balance in the Canadian Rocky Mountains. *International Journal of Climatology*,  
1056 *27*(2), 233–247. <https://doi.org/10.1002/joc.1398>
- 1057 Spicer, R. (1986). Glaciers in the Olympic Mountains, Washington—Present distribution and  
1058 recent variations. [M.S.]. University of Washington.
- 1059 Spicer, R. C. (1989). Recent variations of Blue Glacier, Olympic Mountains, Washington, USA.  
1060 *Arctic and Alpine Research*, *21*(1), 1–21. <https://doi.org/10.2307/1551513>
- 1061 Tangborn, W. V., Fountain, A. G., & Sikonia, W. G. (1990). Effect of area distribution with  
1062 altitude on glacier mass balance—a comparison of North and South Klawatti Glaciers,  
1063 Washington State, USA. *Annals of Glaciology*, *14*, 278–282.
- 1064 Thompson, D. W. J., & Wallace, J. M. (1998). The Arctic oscillation signature in the wintertime  
1065 geopotential height and temperature fields. *Geophysical Research Letters*, *25*(9), 1297–  
1066 1300. <https://doi.org/10.1029/98GL00950>

1067 Thompson, D. W. J., Wallace, J. M., Kennedy, J. J., & Jones, P. D. (2010). An abrupt drop in  
1068 Northern Hemisphere sea surface temperature around 1970. *Nature*, 467(7314), 444–  
1069 447. <https://doi.org/10.1038/nature09394>

1070 Trenberth, K. E. (1997). The definition of el nino. *Bulletin of the American Meteorological*  
1071 *Society*, 78(12), 2771–2778. [https://doi.org/10.1175/1520-](https://doi.org/10.1175/1520-0477(1997)078<2771:TDOENO>2.0.CO;2)  
1072 0477(1997)078<2771:TDOENO>2.0.CO;2

1073 Trenberth, K. E., & Hurrell, J. W. (1994). Decadal atmosphere-ocean variations in the Pacific.  
1074 *Climate Dynamics*, 9(6), 303–319. <https://doi.org/10.1007/BF00204745>

1075 USDA, 2019. [https://www.fsa.usda.gov/programs-and-services/aerial-photography/imagery-](https://www.fsa.usda.gov/programs-and-services/aerial-photography/imagery-programs/naip-imagery/index)  
1076 [programs/naip-imagery/index](https://www.fsa.usda.gov/programs-and-services/aerial-photography/imagery-programs/naip-imagery/index), accessed March 2017

1077 UW, 2019. <http://gis.ess.washington.edu/data/raster/doqs/index.html>, data referenced  
1078 November 2007

1079 UW, (2018). [research.jisao.washington.edu/datasets/pdo/](https://research.jisao.washington.edu/datasets/pdo/)

1080 Van Vuuren, D. P., Edmonds, J., Kainuma, M., Riahi, K., Thomson, A., Hibbard, K., Hurtt, G. C.,  
1081 Kram, T., Krey, V., & Lamarque, J.-F. (2011). The representative concentration pathways:  
1082 An overview. *Climatic Change*, 109(1–2), 5. <https://doi.org/10.1007/s10584-011-0148-z>

1083 Wallace, J. M., & Gutzler, D. S. (1981). Teleconnections in the Geopotential Height Field during  
1084 the Northern Hemisphere Winter. *Monthly Weather Review*, 109(4), 784–812.  
1085 [https://doi.org/10.1175/1520-0493\(1981\)109<0784:TITGHF>2.0.CO;2](https://doi.org/10.1175/1520-0493(1981)109<0784:TITGHF>2.0.CO;2)

1086 Walters, R. A., & Meier, M. F. (1989). Variability of Glacier Mass Balances in Western North  
1087 America. In *Aspects of Climate Variability in the Pacific and the Western Americas* (pp.  
1088 365–374). American Geophysical Union. <http://dx.doi.org/10.1029/GM055p0365>

1089 WGMS, 2019, <https://wgms.ch/faqs/> data referenced, February 2019.  
1090  
1091 Wood, R. L. (1976). *Men, mules, and mountains: Lieutenant O'Neil's Olympic expeditions*.  
1092 Mountaineers Books.  
1093 Zhang, X., Wang, J., Zwiers, F. W., & Groisman, P. Y. (2010). The influence of large-scale climate  
1094 variability on winter maximum daily precipitation over North America. *Journal of*  
1095 *Climate*, 23(11), 2902–2915. <https://doi.org/10.1175/2010JCLI3249.1>  
1096  
1097

1098 **Appendix**

1099  
 1100 **Uncertainty** Assessment of the interpretation uncertainty evolved over time. For the 1990  
 1101 imagery we followed Spicer (1986) whereby it was visually ranked into three categories: 1)  
 1102 excellent – minimal snow/rock cover or shadows,  $\pm 2.5\%$ ; 2) good - moderate cover or shadows,  
 1103  $\pm 7.5\%$ ; and 3) poor - extensive cover or shadow  $\pm 20\%$ . For the 2009 inventory, each glacier was  
 1104 outlined twice. The first outline included only clean and debris-covered ice as indicated by  
 1105 crevasses. The second outline included exposed ice, debris, and seasonal snow. The  
 1106 interpretation uncertainty is one-half of the difference between the two areas outlined.  
 1107 Although more precise, results did not vary significantly from a broader calibrated assessment  
 1108 we applied to the 2015 inventory. The glaciers were visually grouped into two categories low  
 1109 and high uncertainty. A subset of 37 (low) and 34 (high) glaciers were then outlined using the  
 1110 min/max method. The difference between the minimum and maximum outline was then  
 1111 normalized to the glacier area and an average was calculated for the two groups. The low  
 1112 category had a  $\pm 4\%$  uncertainty, and the high had  $\pm 16\%$  uncertainty.

1113  
 1114 **Table A1.** Comparison of the topographic characteristics for the most and least  
 1115 changed glaciers from the quartile analysis. Elev is elevation, Asp – aspect, Win –  
 1116 winter, Sum – summer, Ann – annual, Temp – air temperature, Precip – precipitation  
 1117 Long – longitude, Lat – latitude, Frac Chg – fractional area change From: Olympic-  
 1118 Wilson-ReAnalysis/Quartile

	Largest fractional change	Standard deviation	Least fractional change	Standard deviation	Upper minus lower
Mean Slope	21	5	23	6	-3
Mean Elev	1612	149	1764	124	-152
Max Elev	1672	159	1923	183	-250
Min Elev	1566	158	1598	181	-32
Mean Asp	207	157	211	144	-5
Win Precip	2697	1019	2655	1035	42
Win Temp	-1.7	0.9	-2.4	0.9	0.7
Sum Temp	9.3	0.8	8.7	0.8	0.6
Ann. Precip	3730	1429	3622	1482	108
Ann Temp	2.8	0.8	2.2	0.8	1
Mean Long	-123.6	0.2	-123	0.2	-0.1
Mean Lat	47.8	0.1	48	0.1	0.0
Mean Area	0.06	0.09	0.56	1.19	-0.50
Mean Frac Chg	-0.98	0.03	-0.37	0.12	-0.61
Number	54		55		

1119  
 1120

1121 **Table A2.** *The area (km<sup>2</sup>) of Blue Glacier used for the mass balance model. The area for the*  
 1122 *years 1915 – 1982 were from Spicer (1989). The area for 1990 – 2015 came from our analysis.*  
 1123 *The area is that of the trunk glacier and does not include the ‘snow dome’ which did not change*  
 1124 *in area over the time observed.*  
 1125

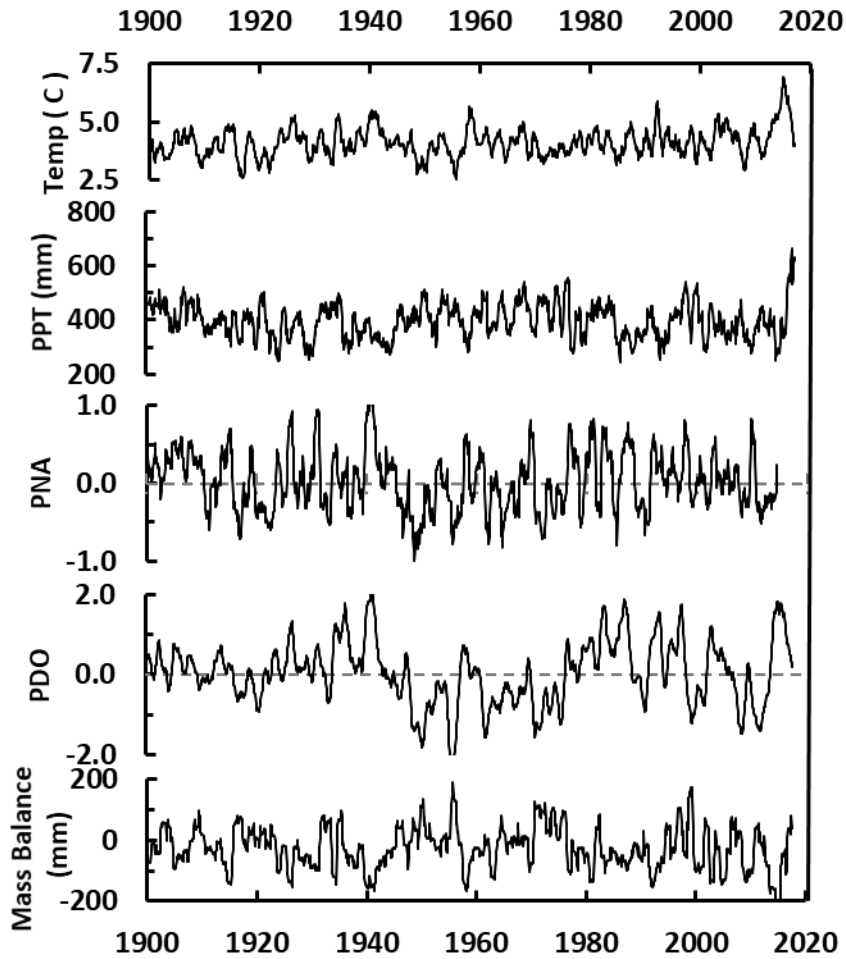
Year	Area
1815	5.98
1900	5.61
1906	5.61
1912	5.61
1913	5.61
1915	5.61
1919	5.61
1924	5.57
1933	5.38
1939	5.31
1952	5.21
1957	5.23
1964	5.22
1965	5.22
1966	5.23
1967	5.23
1968	5.23
1970	5.24
1976	5.30
1977	5.30
1978	5.30
1979	5.31
1981	5.31
1982	5.30
1990	5.08
2009	4.71
2015	4.47

1126  
 1127  
 1128  
 1129  
 1130 **Table A3.** *Correlations between monthly values modeled glacier mass balance, air temperature,*  
 1131 *and precipitation, and various climate indices over the period 1900-2014, all smoothed by a 1-*  
 1132 *year running mean. The bold indicates the highest correlations between the indexes and glacier-*  
 1133 *local measurements. The abbreviations are, ppt –precipitation (mm), temp – average air*  
 1134 *temperature, MB – mass balance, Nino 3.4 – sea surface temperature anomaly in the 3.4 region*

1135 of the Pacific Ocean, PDO – Pacific decadal oscillation, PNA – Pacific North America, SOI –  
 1136 Southern oscillation index, NP – North Pacific. See text for citations and data sources.  
 1137

	<i>ppt</i>	<i>temp</i>	<i>MB</i>	<i>Nino</i> <i>3.4</i>	<i>PDO</i>	<i>PNA</i>	<i>SOI</i>	<i>NP</i>	<i>NAO</i>	<i>Sunspots</i>
<i>ppt</i>	1.00									
<i>temp</i>	-0.12	1.00								
<i>MB</i>	0.52	-0.74	1.00							
<i>Nino 3.4</i>	-0.13	0.52	-0.43	1.00						
<i>PDO</i>	-0.19	<b>0.53</b>	<b>-0.52</b>	0.55	1.00					
<i>PNA</i>	-0.11	<b>0.64</b>	<b>-0.59</b>	0.53	0.66	1.00				
<i>SOI</i>	0.15	-0.47	0.40	-0.83	-0.54	-0.47	1.00			
<i>NP</i>	0.15	<b>-0.58</b>	<b>0.56</b>	-0.45	-0.58	-0.71	0.48	1.00		
<i>NAO</i>	0.08	0.05	0.05	0.04	0.01	-0.15	-0.11	0.18	1.00	
<i>Sunspots</i>	-0.04	0.09	-0.11	0.03	-0.06	-0.08	0.01	-0.05	0.15	1.00

1138  
 1139  
 1140  
 1141  
 1142  
 1143  
 1144  
 1145



1146

1147

1148

1149

1150

**Figure A1.** Smoothed time series (1 year) of monthly local air temperature, precipitation, two climate idiocies (PNA – Pacific North America; PDO – Pacific Decadal Oscillation) and modeled glacier mass balance.